 doi:10.20944/preprints202210.0212.v1

Catalytic Hydrolysis of Organophosphorus Nerve Agents by Metal-organic Frameworks: What Happens Next?

Yunzhuo Li[1]

[1]**Weinberg College of Arts and Sciences, Northwestern University, 633 Clark Street, Evanston, IL, 60201; timli2026@u.northwestern.edu**

Abstract

Organophosphorus nerve agents are amongst the most toxic chemicals known to human beings. They interfere with the central nervous system, resulting in continuous muscle contractions, paralysis and even death. Prohibition by many countries around the world cannot disguise the remaining presence of nerve agents in stockpile storage and governmental deployment, highlighting the dire need for an efficient catalyst to degrade and detoxify nerve agents by hydrolysis. Metal-organic frameworks (MOFs) have raised a few eyebrows for their permanent porosity, precise tunability, and lasting stability. Modern Reticular Chemistry fosters the design and synthesis of well-defined crystalline MOFs with open Lewis acidic metal sites that can catalytically hydrolyze nerve agents both in aqueous solution and in solid state systems, unveiling unparalleled potential for MOF-based personal protection gears. In this review, a summary of the representative catalytically active MOFs in nerve agent hydrolysis is discussed. MOFs are categorized by their reticular structure, emphasizing the capability and mechanistic insights of each single MOF in nerve agent hydrolysis. The author's perspective on the current challenges and future directions of MOF-based catalysts in real-world protection applications is also provided, which hopefully could shed some light on the future development of commercially available MOF protection suits.

Keywords: Metal-organic frameworks; chemical warfare agents; catalytic hydrolysis

1. Introduction

When people are introduced to the concept of chemical warfare agents (CWAs), the very first

Preprints (www.preprints.org) | NOT PEER-REVIEWED | Posted: 14 October 2022 doi:10.20944/preprints202210.0212.v1

thing that pops up would probably be the large-scale deployment of lethal chemical weapons--such as phosgene and sulfur mustard gas--in World War I[1]–[4]. While the German deployment of chlorine gas in April 1915 did render catastrophic outcomes, it is worth noting that World War I was not the first time that CWAs were applied to cause casualties. The earliest application of CWAs dates to Ancient Roman times when Hannibal Barca ordered the Carthaginian troops to fire jars of poisonous snakes at the Roman battleships in 190 BCE[5].

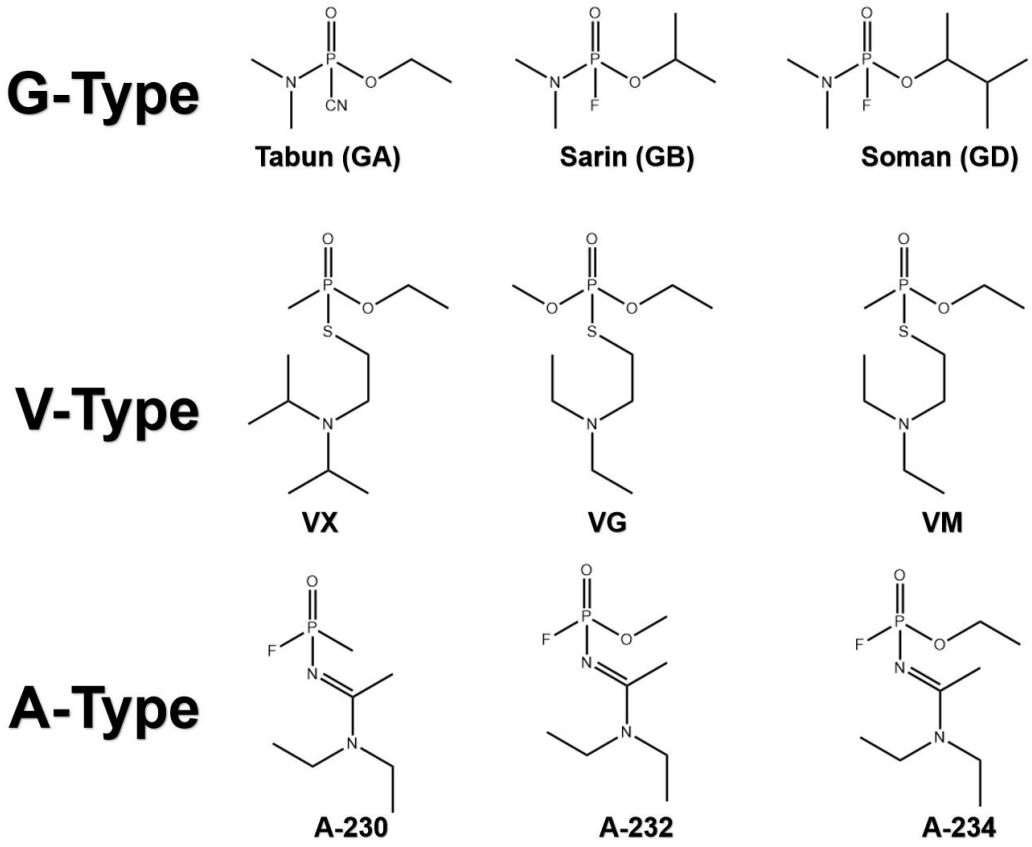

Figure 1.1 Structures of common nerve agents including G-type, V-type and A-type.

The Carthaginian legend probably did not foresee that after 2 millennia, his strategy was again adopted, but with a more fatal fashion. After World War I and before World War II, extremely toxic organophosphorus nerve agents were discovered. As illustrated in **Figure 1.1**, Nerve agents are organophosphorus compounds and are typically structural variations of phosphoric acid esters. In 1936, when Gerhard Schrader was in search of new pesticides, he successfully synthesized many organophosphorus compounds, including the highly toxic ethyl-N,N-dimethylphosphoramidocyanidate (Tabun, GA) and isopropyl methylphosphonofluoridate (Sarin, GB)--both fatal nerve agents [6] . Fortunately, lethal nerve agents Tabun and Sarin were not deployed in World War II, otherwise much severer casualties could have been rendered [4] . Nevertheless, the discovery of new nerve agents went on. Later in 1944, Pinacolyl methylphosphonofluoridate (Soman, GD) was synthesized by the Austrian-German Nobel laureate chemist Richard Kuhn [7] . Meanwhile, V-class nerve agents were identified by US and British laboratories. Amongst these V-type nerve agents, o-ethyl-S-(2-diisopropylamino-ethyl)-methyl-phosphonothiolate (VX) was deemed arguably as the most lethal CWA ever discovered [8], [9] .

Preprints (www.preprints.org) | NOT PEER-REVIEWED | Posted: 14 October 2022 doi:10.20944/preprints202210.0212.v1

Furthermore, a 1994 report revealed the synthesis of "Novichok" nerve agents (meaning "newcomers' in Russian), which are organophosphates containing a dihaloformaldoxime moiety[10]. These Novichok agents, also referred to as the A-type agents, are hard to degrade and could be reportedly 5-8 times more potent than VX [11] . Regardless of the type, all the nerve agents directly interfere with the operation of the central nervous system by covalently binding to the active site of acetylcholinesterase, an enzyme responsible for regulating choline ester-based neurotransmitters that are essential to voluntary control of muscle contraction, inhibiting the enzyme from functioning properly. This inhibition results in the buildup of the neurotransmitter acetylcholine and, subsequently, continuous muscle contractions, ultimately leading to paralysis and death[12], [13].

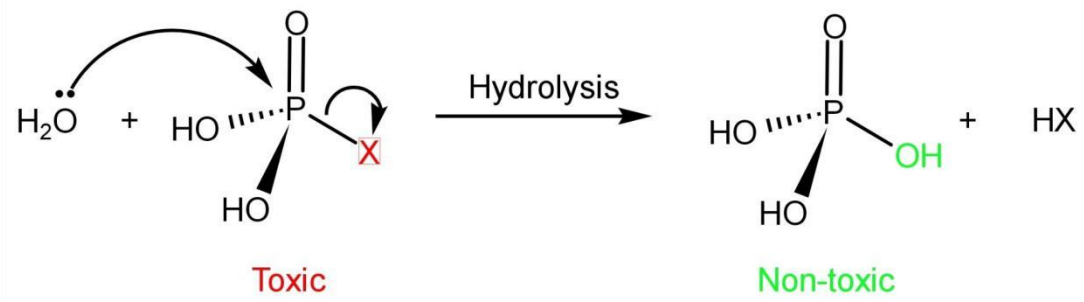

Figure 1.2 Hydrolysis pathway of common nerve agents involving P-X moieties.

These nerve agents are not far away from us. Syrian government forces repeatedly attacked civilians with sarin nerve gas and killed as many as 1,400 civilians in a single attack [14], [15] . More recently, Kim Jong Nam fell victim of the nerve agent in Malaysia, dying only a few minutes after exposure to VX[9]. Novichok was used in an assassination attempt against a former Russian military intelligence officer in the United Kingdom on March 4th 2018[16], and was most recently employed in 2020 in Russia [17] . Some have even identified the possibility of Russian Federation using nerve agents to aid its recent invasion of Ukraine [18] . Moreover, organophosphorus nerve agents do not require harsh conditions to synthesize [19] . These facts highlight the need not only for destroying stockpile nerve agents, but also for personal protection gears to prevent inhalation of them. In both cases, the essence is to cope with organophosphorus nerve agents' dreadful toxicity and 'degrade' them by chemical reactions, turning them from something that takes away lives to something that human bodies could tolerate. Amongst all the strategies that attempt to degrade organophosphorus nerve agents, hydrolysis is among the most effective in decreasing their toxicity. In a typical hydrolysis reaction, the OH^- (or water) serves as a nucleophile and attacks the central atom [20], [21] . As shown in **Figure 1.2**, the key to the hydrolysis reaction lies behind the P-X single bond (where X is -Cl, -F, -OR etc.), which could serve as a leaving group in nucleophilic substitution. When the nucleophile attacks the phosphorus central atom, the P-X bond cleaves and -X is replaced by a hydroxyl group. This process resembles the S_N2 reaction in Organic Chemistry [22], [23] , except for the central atom being phosphorus instead of carbon.

Early efforts dedicated towards destroying the stockpile nerve agents include the use of strong base solutions, such as sodium hydroxide (NaOH) and potassium hydroxide (KOH) [24] . The

Preprints (www.preprints.org) | NOT PEER-REVIEWED | Posted: 14 October 2022 doi:10.20944/preprints202210.0212.v1

nerve agents dissolved in the solutions could be immediately hydrolyzed. However, these base solutions bare poor stability in air and are not suitable for long-term storage. Their activities decrease as the hydrolysis proceeds due to a fall in the concentration of hydroxide ions in the solution. Most importantly, these bases are themselves highly corrosive and are unrealistic to be incorporated into a personal protection gear [25]. An alternative approach is to decompose nerve agents at very high temperatures, whereas this method leads to the formation of gaseous pollutants and is also not suitable for personal protection [26]. These considerations propelled the catalytic hydrolysis method, which most commonly utilizes Lewis acidic sites to prompt the hydrolysis of nerve agents. When the phosphoryl oxygen of a nerve agent molecule binds to a Lewis acid, the oxygen atom is activated by donating electrons to the Lewis acid. The phosphorus atom therefore also becomes electron deficient and more susceptible to nucleophilic attack. One source of inspiration for the design of Lewis acid catalysts stemmed from the Zn(II) ions at the active sites of a series of enzymes such as phosphotriesterase, methyl parathion hydrolase (MPH), and paraoxonase 1 (PON1) [27]–[30] . These enzymes rely on metal-oxy/hydroxy (M-O/M-OH) moieties to achieve the catalytic hydrolysis of nerve agents. Still, these enzymes bare poor stability and are easily 'poisoned' and denatured[31], deterring them from real-world applications. Catalysts that entail both high efficiency and excellent stability is thus in a dire time of need. A class of porous material encompassing both Lewis acidic sites and rigid structures have raised a few eyebrows: metal-organic frameworks (MOFs).

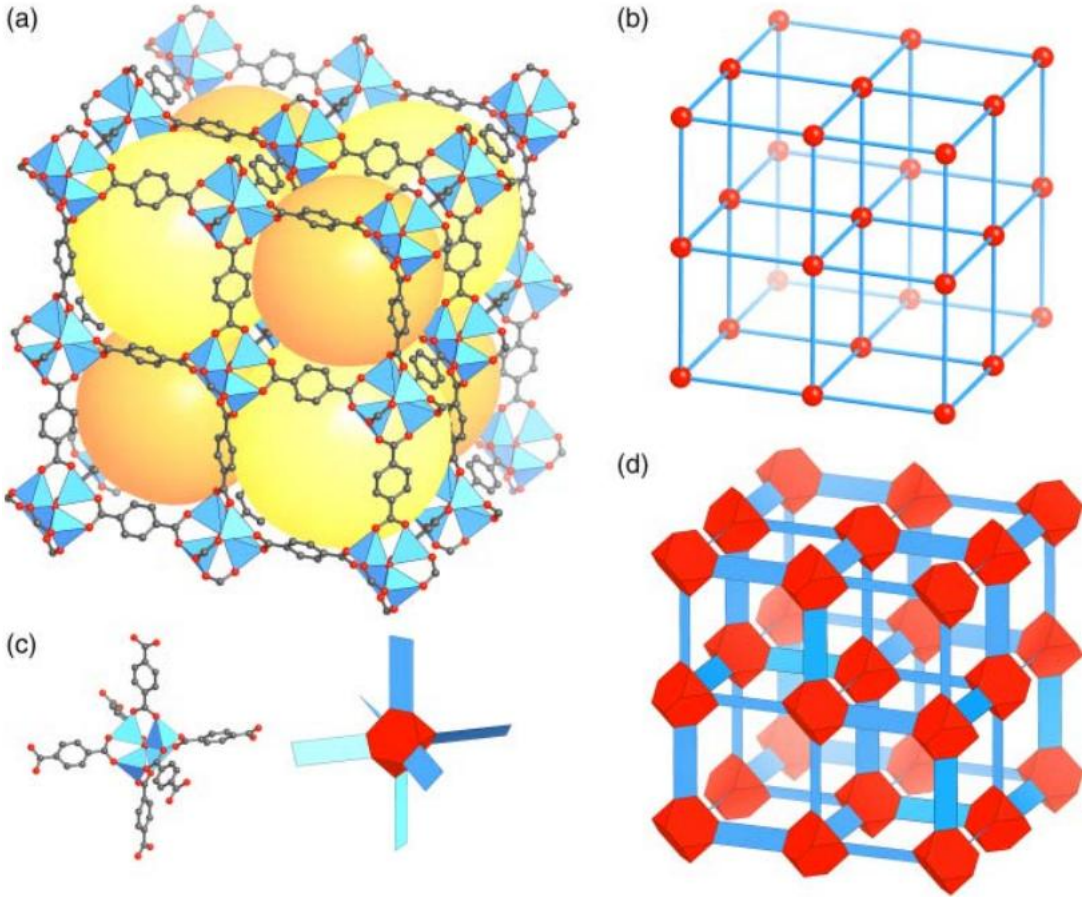

Figure 1.3 (a) Crystal structure of MOF-5, the earliest MOF synthesized and among one of the most well-known MOFs. Color code: Zn (blue tetrahedra), C (gray), O (red). (b) Simplified representation of the basic pcu net of MOF-5. $Zn_4O(\text{-}COO)_6$ SBUs are replaced by red spheres

Preprints (www.preprints.org) | NOT PEER-REVIEWED | Posted: 14 October 2022 doi:10.20944/preprints202210.0212.v1

resembling iron balls and the terephthalic acid linkers are replaced by blue lines resembling bar magnets. (c) Envelope representation of the octahedral SBUs and the linkers as truncated tetrahedra and rectangles, respectively. (d) Envelope representation of the extended framework structure of MOF-5. Figure adapted from **Figure 1.17** on page 23 of reference [32]. Adapted with permission. © 2019 Wiley - VCH Verlag GmbH & Co. KGaA.

MOFs are porous crystals consisting of inorganic metal-oxo clusters and organic ligands[32], [33]. As shown in **Figure 1.3**, these inorganic and organic building units fit together like little iron balls and bar magnets to form various extended structures (more vividly, may be referred to as 'tinker toy'). MOFs are outstanding materials due to their variability, tunability, and functionality. The individual metal ions are gathered by the bridging oxygen and hydroxide ions to form metal clusters, namely the secondary building units (SBUs), which are further connected by organic molecules (linkers) to form an extended structure [32], [34] . An SBU is like a repertoire of the readily accessible Lewis acidic sites [35] . There are also terminating -OH and -OH_2 groups coordinating to the metal ions, forming metal-oxy/hydroxy (M-O/M-OH) moieties resembling those on the enzymes that could catalyze the hydrolysis of nerve agents [36]–[38] . Furthermore, removing organic linkers in the lattice of MOFs introduces structural defects at the SBUs, resulting in larger exposure of the metal ions and higher Lewis acidity [39], [40] . MOFs that are stable in water and a wide pH range have also been reported [41], [42] . Moreover, MOFs have ultrahigh specific surface area, which is beneficial for the absorption of nerve agents into their pores[32].

This review article aims to briefly summarize the current progress on the catalytic hydrolysis of nerve agents using MOFs. Due to limited data and relatively scarce research related to the hydrolysis of A-type Novichok agents, this review mainly focuses on MOFs' catalytic hydrolysis of G-type and V-type nerve agents (and their simulants). Because of the hefty amount of research and rapid advancement in this topic, this review does not aim at providing a comprehensive list of all the MOFs that could serve as catalysts for nerve agent hydrolysis. Instead, an overview of the prominent examples in each family of MOFs (divalent, trivalent, and tetravalent) is provided, with an emphasis on the mechanistic insights and design rules that have been developed. This review also offers insights into the current limitations and considerations for existing MOF nerve agent hydrolysis catalysts, and how future generations of these materials could be improved to meet the need for personal protection masks.

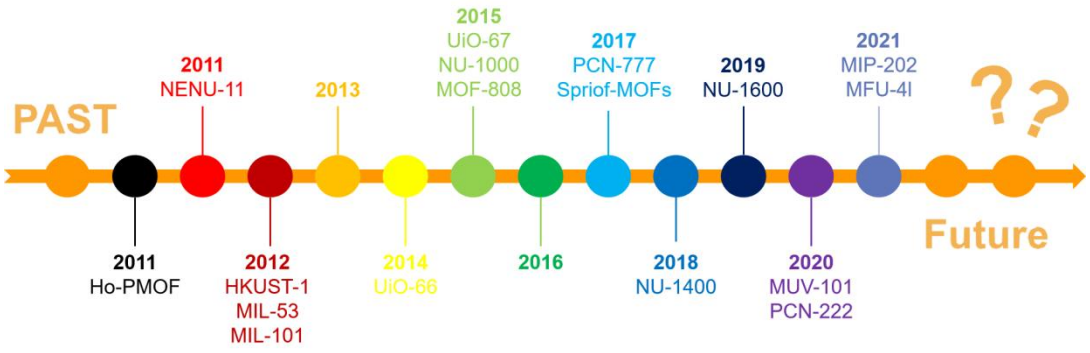

 doi:10.20944/preprints202210.0212.v1

Figure 1.4 Timeline of when certain representative MOFs were FIRST reported to be able to catalyze the degradation of nerve agent (simulants).

2. General Experimental Strategies

Because the actual nerve agents are rather detrimental to the human body, only trained and qualified personnel could carry out experiments with them [25] . In a common laboratory where such qualification is limited, nerve agent simulants are usually used to take the place of the actual nerve agents[43]. These nerve agent simulants have similar functionalities to real nerve agents, but they are less detrimental because the P-X bond in a real nerve agent molecule is replaced by the relatively noble P-OR bond[43], [44]. In most cases, the reactivity of a nerve agent closely mimics that of its simulant, and they undergo the same pathway for hydrolysis. As the examples shown in **Figure 2.1 (A)** and **(B)**, the hydrolysis of a standard nerve agent simulant dimethyl p-nitrophenyl phosphate (DMNP) in the presence of a Lewis acidic catalyst yields dimethyl hydrogen phosphate and 4-nitrophenol demonstrating similar reactivity to many G series agents[45]. The 4-nitrophenyl acts as the de facto leaving group in DMNP hydrolysis, just like the -F leaving group in a real Soman molecule[45]. However, it should be noted that the nerve agent simulants could not mimic every aspect of a real nerve agent. In the hydrolysis of VX shown in **Figure 2.1 (C)**, two outcomes are possible: the cleavage of P-S bond when pH is smaller than 6 or greater than 10, and the cleavage of P-OR bond when pH is between 7 and 10. In the latter case where the P-OR cleavage resembles the hydrolysis pathway of nerve agent simulants, EA-2192 also a highly toxic chemical to human beings, is produced[45], [46]. The 2 hydrolysis products of VX, therefore, emphasize the potential discrepancy between the hydrolysis of a real nerve agent and its simulant that must be cautioned when changing the target hydrolysis reactant to nerve agent simulants in the lab to actual nerve agents in real-world applications.

Preprints (www.preprints.org) | NOT PEER-REVIEWED | Posted: 14 October 2022 doi:10.20944/preprints202210.0212.v1

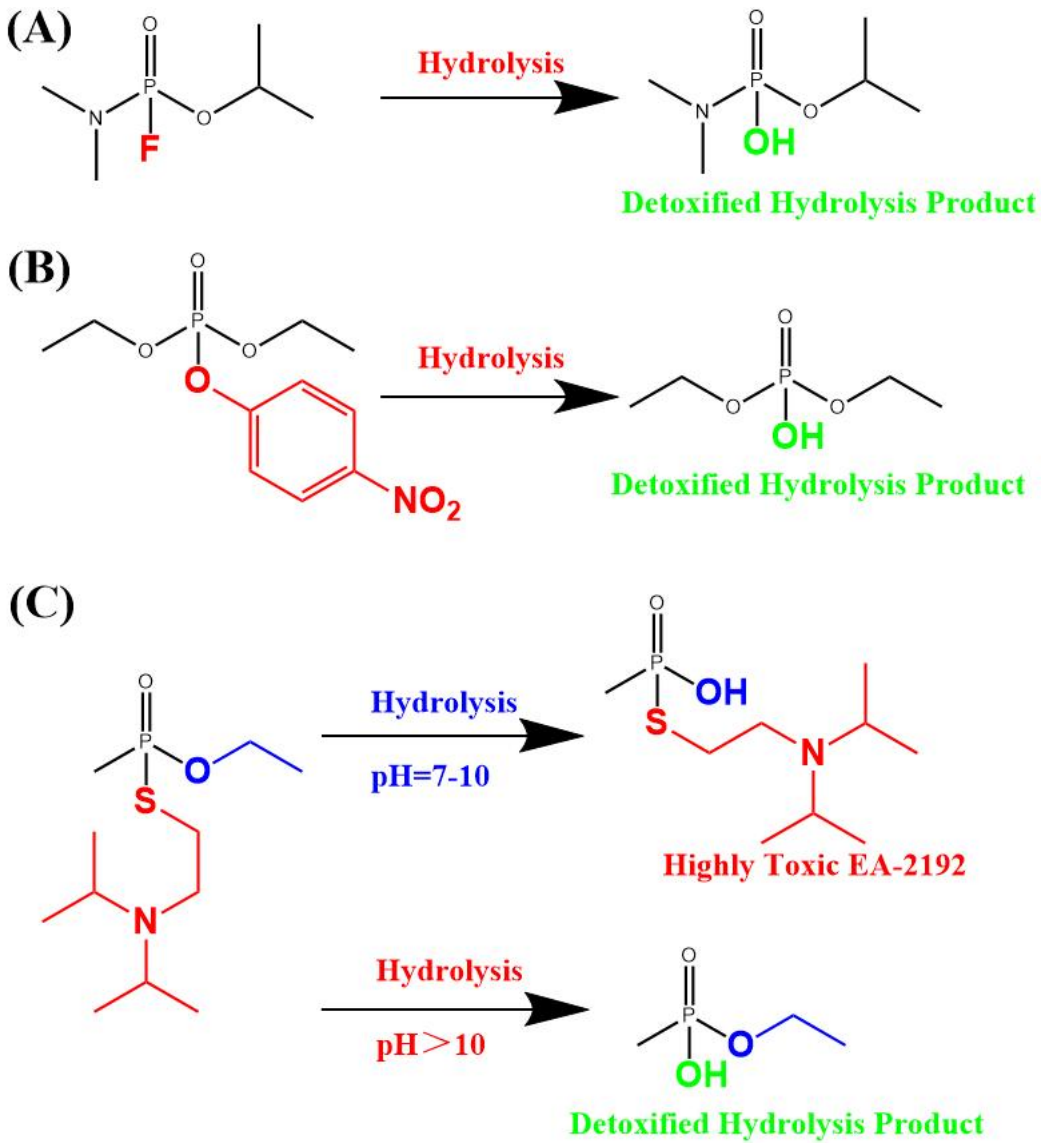

Figure 2.1 Specific examples of nerve agent hydrolysis. **(A)** Hydrolysis of the actual nerve agent GD in the presence of a Lewis acid catalyst; **(B)** hydrolysis of nerve agent simulant (DMNP) in the presence of a Lewis acid catalyst; and **(C)** two potential outcomes of the hydrolysis of nerve agent VX, one of which producing the toxic EA-2192[45].

The mechanism for the hydrolysis of nerve agents and their simulants, as stated in the Introduction section, is similar to that of an SN_2 reaction, where the -X (-X could either be halogens or -OR) group is replaced by the -OH group. Therefore, to increase the rate of reaction by a Lewis acid catalyst, the accessibility of the Lewis acidic sites should be the very first priority considered[47]. The easier for nerve agent molecules to reach and bind the metal ions on the SBUs, the faster the reaction proceeds. MOFs should thus be designed and synthesized to have (1) large pore sizes and pore openings; (2) precisely-introduced defect sites; (3) small number of linkers connected to the metal nodes; and (4) small crystal sizes (nanoMOFs) to enhance the availability of exposed metal ions and allow nerve agent (simulant) molecules to access more Lewis acidic metal sites, leading to enhanced catalytic activity. Details of MOFs' design strategies will be discussed in Section 6.

 doi:10.20944/preprints202210.0212.v1

Besides the accessibility of the Lewis acidic metal ions, a basic condition needs to be maintained throughout the reaction process to ensure sufficient hydroxide ions present in the reaction solution. In the lab, a typical catalytic reaction would involve 3−6 mol % MOF loading into a UV-vis vial or NMR tube (to monitor the reaction in-situ), followed by the addition of an aqueous solution containing the nerve agent simulant and a base--which keeps the pH value of the solution at around 10 [43]. This is to prompt the nucleophilic attack of the organophosphorus substrate, as well as to remove acidic byproducts from the reaction (e.g., HF following the hydrolysis of Soman). Choosing the right base is therefore of great importance in achieving the efficient hydrolysis of nerve agents. Early options of bases include homogeneous bases such as N-ethylmorpholine and trimethylamine. These bases constitute basic buffer solutions, sacrificing themselves to help hydrolyze nerve agents [48]. However, these small molecule bases are highly volatile, and their inhalation could pose safety implications [48]. Garibay et al have attempted to functionalize the modulators used in MOFs' synthesis with these volatile bases, aiming to 'anchor' these small molecules onto the SBUs; however, these amino-functionalized modulators may separate from the SBUs after several cycles of reaction, leading to poisoning and a fall in catalytic activity [49]. Apart from the small molecule homogeneous bases which dissolve in the solution, heterogeneous polymeric bases have raised a few eyebrows for their potential to be incorporated into personal protection gears[43], [45], [47], [48]. These base polymers include poly(amidoamine) dendrimers (PAMAM), as well as branched and linear polyethylenimine polymers (B-PEI and L-PEI), which have all demonstrated comparable performance in the catalytic hydrolysis of nerve agents with the small molecule bases. Still, hydrolysis reactions based on solid non-volatile bases suffer from relatively sluggish kinetics due to limited interaction between the base macromolecules and the MOF catalyst.

Selecting the right MOF that has both ultrahigh water stability and water-capturing capabilities at low relative humidity is also crucial. In the lab, the hydrolysis reactions of nerve agents are typically carried out under aqueous conditions rich in water. However, inside personal protection gears with no external water supply, exhalation becomes the only source for water molecules. Yaghi et al have proven that many MOFs are promising candidates for water harvesting at low relative humidity [50], [51], so it should be not too hard to choose a MOF that could rely on the steam from exhalation to satisfy the water needed for hydrolysis. Moreover, compositing MOF with a hydrogel could increase local water concentration and resolve water scarcity in solid-state catalytic systems [52]. Heterometallic MOFs that combine the properties of various metal ions are also promising materials in nerve agent hydrolysis [53]–[55], as we will discuss in more detail in Section 4.

Preprints (www.preprints.org) | NOT PEER-REVIEWED | Posted: 14 October 2022 doi:10.20944/preprints202210.0212.v1

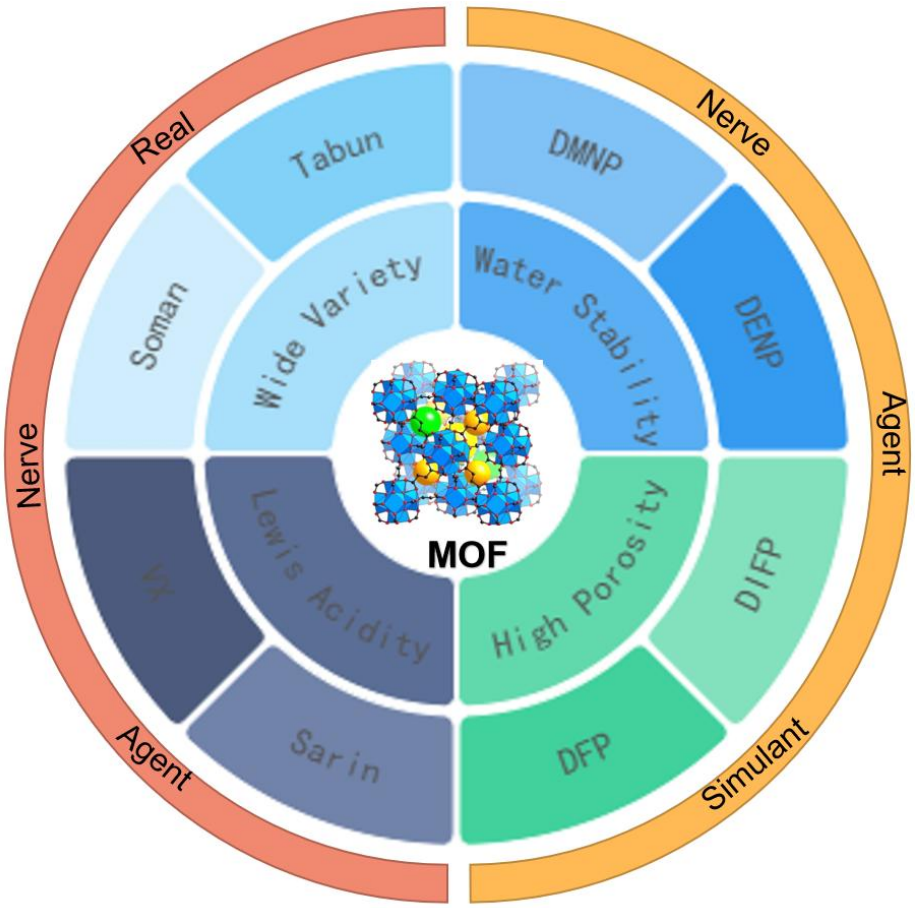

Figure 2.2 Properties of MOFs that make them promising for the catalytic hydrolysis of various nerve agents and simulants.

3. Divalent MOFs as Catalysts for Nerve Agent Hydrolysis

Before discussing some of the earliest examples of divalent MOF catalysts, we need to distinguish between the absorption of nerve agents and their degradation. Among the first discovered and most popular MOFs in the world, MOF-5 shown in Figure 1.3 have been demonstrated to be a promising material to absorb and capture the G-type nerve agent Sarin, as well as mustard gas (which are beyond the scope of this review)[56]. Moreover, the absorption capacity of MOF-5 for the nerve agent simulant DMMP could reach 6 molecules per SBU. Though effective at absorbing the nerve agent and its simulant, MOF-5 could not catalyze their hydrolysis. One of the prerequisites for MOF catalysts is the capability to catalyze the hydrolysis reactions, so that the MOFs do not get worn out and could be recycled for long-term usage in real life[57].

Preprints (www.preprints.org) | NOT PEER-REVIEWED | Posted: 14 October 2022 doi:10.20944/preprints202210.0212.v1

3-1. NENU-11

One of the earliest examples of an effective MOF catalyst dates back to 2011, when NENU-11, synthesized from the polyoxometalate Keggin-type anion $[PW_{12}O_{40}]^{3-}$ (**Figure 3.1)**, was demonstrated to effectively absorb and degrade the G-type nerve agent simulant DMMP [58] . Polyoxometalates (POMs) are polyoxoanions of the early transition elements[59], whose manifold structural symmetries could direct the formation of MOF crystals. Therefore, MOFs synthesized using POMs as templates, NENU-11 included, are called PMOFs. This PMOF is built from the square planar SBU with a Cl atom at the center and four Cu ions at 4 corners, and trimesic acid (BDC) organic linkers shown in **Figure 3.1 (b)** and **(c)**. Each SBU connects with 8 linkers, and each linker in turn connects with 3 SBUs. Oriented by the Keggin-type anion, NENU-11 crystallizes in an Fm3m face-centered cubic space group illustrated in **Figure 3.1 (d)** just like that of the UiO-66 (vide infra). In an SBU, each Cu ion is 5-coordinated (coordinated with 4 oxygen atoms from 4 vicinal linkers and 1 chlorine atom at the center), resulting in coordinative unsaturation because Cu ions tend to form octahedral 6-coordinated geometry. Therefore, each Cu ion tends to accept a lone-pair of electrons, which could serve as a Lewis acidic site. Its Lewis acidity, along with its Cu-O moieties resembling that on the enzymes, make NENU-11 a reasonable candidate for nerve agent hydrolysis.

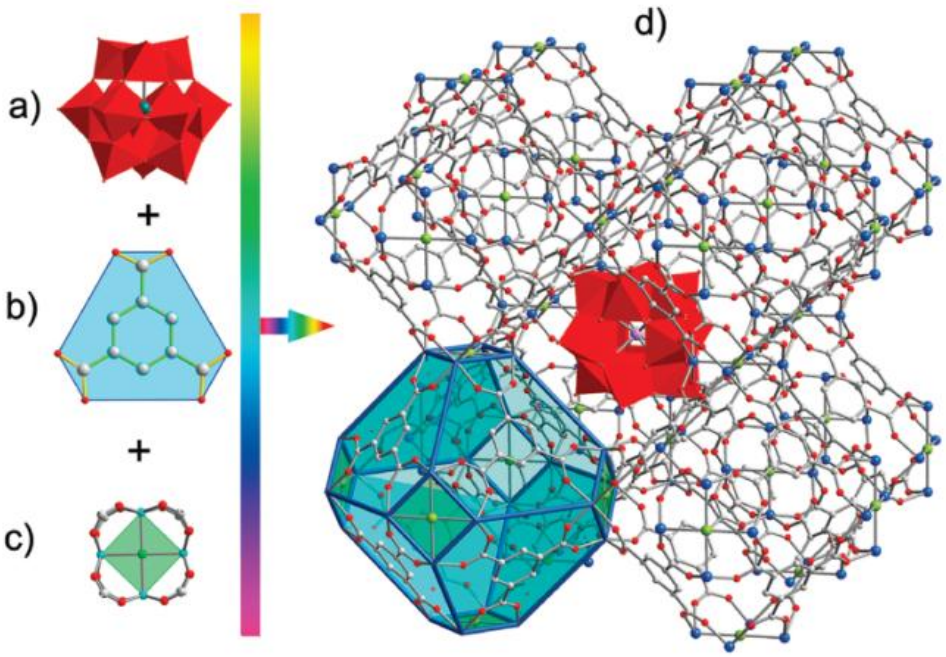

Figure 3.1 (a) Keggin polyanion. **(b)** 3-connected trimesic acid linker **(c)** 8-connected SBU with 4 Cu ions at 4 corners and a chlorine atom at the center. Each Cu ion is coordinatively unsaturated and require an extra dative covalent bond to form the stable octahedral complex **(d)** Fm3m space group and the face-centered cubic geometry of NENU-11. Hydrogen atoms are omitted for clarity. Color code: Cu (blue), O (red), C (gray), Cl (green), Keggin-type polyanion (red polyhedron). Adapted from **Figure 1** of reference[58]. Adapted with permission. Copyright © 2011, American Chemical Society.

Preprints (www.preprints.org) | NOT PEER-REVIEWED | Posted: 14 October 2022 doi:10.20944/preprints202210.0212.v1

After 8 hours of hydrolysis reaction under room temperature, 34% of the DMMP is hydrolyzed. The conversion rate increases to 83% as the temperature rises to 323 K. The half life (the time it takes to hydrolyze the reactant to half of its original concentration) for DMMP hydrolysis of this MOF under room temperature, calculated from the rate equations of the first-order reaction with respect to DMMP concentration, is over 13.3 hours. Though not a very low value, this half-life demonstrates the effectiveness of NENU-11 as a proof-of-concept catalyst for nerve agent hydrolysis. The catalytic activity of NENU-11 is originally attributed to the Keggin anions-which had been utilized as catalysts for ester hydrolysis. Further studies, on the other hand, show that the unsaturated Lewis acidic Cu ions, as suggested in this review, also play a part in catalyzing the hydrolysis reaction.

3-2. HKUST-1

Not long after NENU-11, HKUST-1 was also found to be efficient at the hydrolysis of Sarin[60]. HKUST-1 (HKUST stands for Hong Kong University of Science and Technology) is built from the same copper metal ions and BTC organic linkers as NENU-11, but they have distinct structures, and HKUST-1 could be synthesized from a template-free solvothermal strategy [36] . This is because HKUST-1 has SBUs taking the shape of a paddle-wheel. As shown in Figure 3.2, there are two Cu ions in an SBU, each coordinated to four oxygen atoms on four BTC ligands to form a 4-connected SBU structure. There is also local coordinative unsaturation at Cu ions, which could serve as Lewis acidic sites for nerve agent hydrolysis.

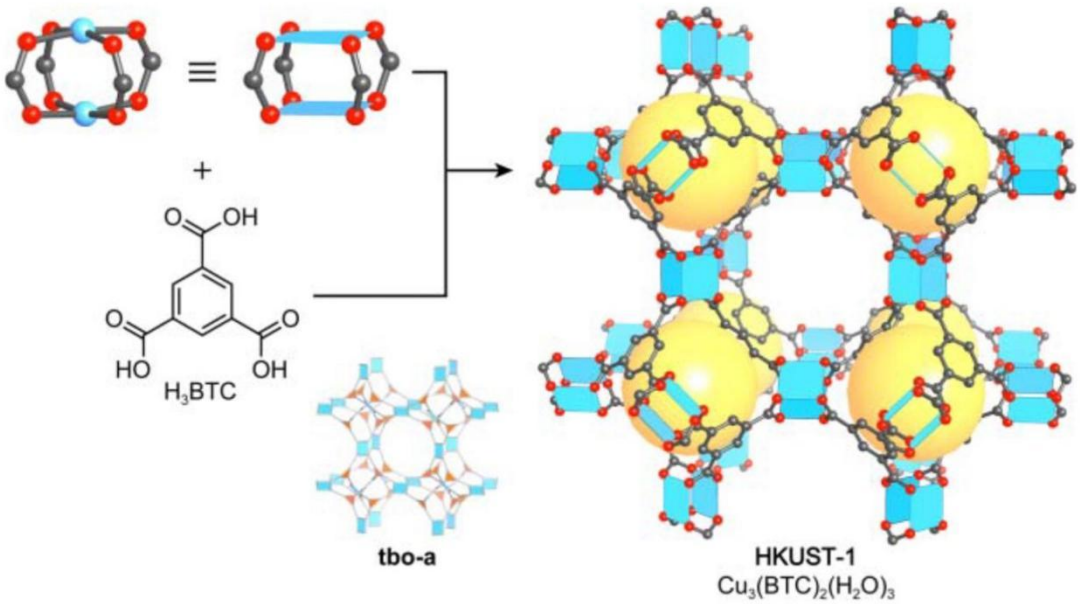

Figure 3.2 The structure of HKUST-1 built from 4-connected paddle-wheel $Cu_2(\text{-}COO)_4$ SBUs and BTC ligands. All hydrogen atoms are omitted for clarification. Color code: Cu (blue), O (red), C (gray). Adapted from **Figure 4.9** on page 89 of reference[32]. Adapted with permission. © 2019 Wiley - VCH Verlag GmbH & Co. KGaA.

The catalytic activity of HKUST-1 is likely to be largely dependent on external conditions, as

Preprints (www.preprints.org) | NOT PEER-REVIEWED | Posted: 14 October 2022 doi:10.20944/preprints202210.0212.v1

different researchers have made significantly distinct observations on the half-life for the catalytic hydrolysis of Sarin (GD). In the research published in 2012, Roy et al illustrated that HKUST-1 showed a half-life for the hydrolysis of Sarin of less than an hour manifested by GC-MS[60]. This half-life value is an order of magnitude higher than that achieved in NENU-11. In this work, HKUST was found to be even more efficient at catalyzing the hydrolysis of two GD simulants--diethylchlorophosphate (DEClP) and diethylcyanophosphonate (DECNP) imitating the nerve agents with -Cl and -CN as leaving groups--reaching half-lives as low as and in due order. The faster hydrolysis rate of DECNP and DEClP could be rendered by the better leaving tendency of -CN and -Cl compared with -F in Sarin. Steric hindrance also plays a part, where the rate of DECNP hydrolysis is faster than that of DEClP due to smaller molecular size and diffusion barrier. However, another study published a year later unveiled different observations. ^{31}P-NMR allowed Peterson and Wagner to precisely track the hydrolysis process, and they suggested in 2014 that the hydrolysis of Sarin catalyzed by HKUST-1 has a half-life as long as 2 days indicated by the disappearance of the left portion of the doublet at 29.6 ppm--characteristic peak for Sarin [61] . Moreover, the hydrolysis of VX using HKUST-1 is approximately 29 hours inferred from the slow disappearance of the VX characteristic peak at 54 ppm. These large values of half-lives, contradictory to the previous observations, may provide evidence that the catalytic hydrolysis of nerve agents by HKUST-1 might be largely dependent on external factors, and a minor change in the reaction condition could result in a tremendous shift in the reaction rate. For example, Roy et al employed dichloromethane as the solvent for the reaction, while Peterson and Wagner adopted a solvent-free strategy, an important difference in the reaction condition which could lead to large deviations in hydrolysis rate.

3-3. MFU-4l

One of most efficient divalent MOFs in catalyzing the nerve agent hydrolysis is Zn-MFU-4l, which is a Zn-triazole MOF constructed with 6-connected Zn_5 nodes and bis(1*H*-1,2,3-triazolo-[4,5-b], [4',5'-i])dibenzo-[1,4]-dioxin (H_2-BTDD) linkers[62]–[64]. The inspiration stemmed from the enzyme carbonic anhydrase (CA), which could be used as a catalyst for phosphonate ester hydrolysis due to its Zn(II)-OH active sites [63] . In the pristine MFU-4l, as shown in **Figure 3.3 (c)**, one Zn ion adopts a stable 4-coordinated tetrahedral coordination geometry, forming three Zn-N dative covalent bonds with three distinct imidazole rings and one Zn-Cl bond with a chlorine atom. The combination of soft Lewis acidic Zn(II) and soft Lewis basic triazole-based building blocks on the linkers of MFU-4l yields a heterogeneous catalyst suitable for the Sarin and DMNP hydrolysis. Indeed, when MFU-4l reaches a weight percentage of 6%, more than 80% of the DMNP is degraded in 3 minutes, which shows a half-life of less than one minute according to the first-order kinetics. This value is among the lowest values of DMNP hydrolysis half-life reported up to date. The half-life for the hydrolysis of Sarin is 3.3 minutes, low enough for MFU-4l to be considered promising for real-world applications. Besides the commonly used N-ethylmorphine buffer solution, the authors also carried out experiments with the heterogeneous base PANAM dendrimers, showing similar reaction rates.

However, possibly intuitively, the Zn-Cl bond is not actually the functional group accountable for

Preprints (www.preprints.org) | NOT PEER-REVIEWED | Posted: 14 October 2022 doi:10.20944/preprints202210.0212.v1

the catalytic activity of MFU-4l. Instead, there must be something resembling the Zn(II)-OH active sites on the enzyme CA. Diffuse reflectance infrared Fourier transform spectroscopy (DRIFTS) proved the existence of the replacement of -Cl by -OH shown in **Figure 3.3 (d)** and **(e)**, the functionality that mimics that on the CA and is responsible for the catalytic activity of MFU-4l[64].

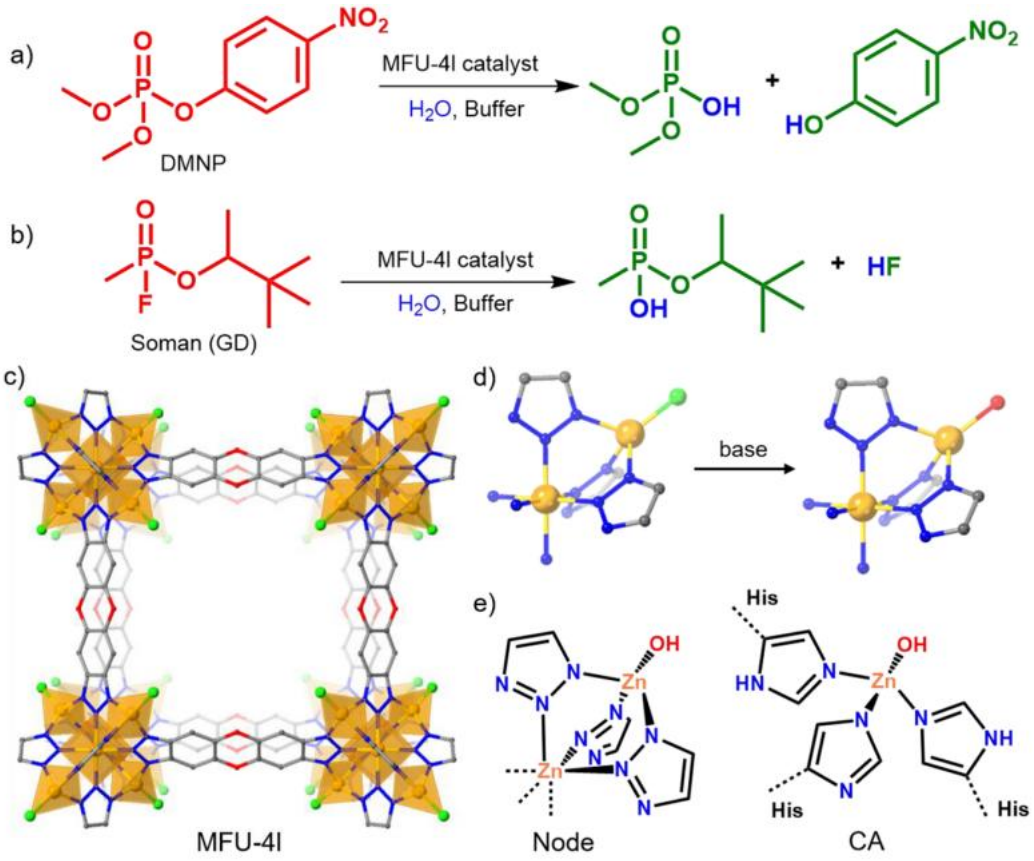

Figure 3.3 Hydrolysis reaction of **(a)** the phosphonate-based nerve agent simulant DMNP (dimethyl (4-nitrophenyl) phosphonate) and **(b)** the real nerve agent GD (O-pinacolyl methylphosphonofluoridate). **(c)** Structural representation of MFU-4l. **(d)** Cl^- ion is replaced with OH^- after base treatment. **(e)** Comparison between the active site in MFU-4l and carbonic anhydrase (CA). All the hydrogen atoms are omitted for clarity. Color code: Zn (brown), Cl (green), C (gray), N (blue) and O (red). Adapted from **Figure 1** of reference [63]. Adapted with permission. Copyright © 2021, American Chemical Society.

4. Trivalent MOFs

4-1. Ho(III) PMOF

A one-dimensional PMOF based on the lanthanide metal Ho(III) was among the first ever reported prototype of a MOF catalyst for nerve agent hydrolysis [65]. In this Ho-PMOF, there is only one Ho(III) ion in a metal node. As shown in **Figure 4.1** the structure of Ho-PMOF, four Ho(III) ions

Preprints (www.preprints.org) | NOT PEER-REVIEWED | Posted: 14 October 2022 doi:10.20944/preprints202210.0212.v1

in the same plane are bridged by four 4,4'-bipyridine-N,N'-dioxide hydrate (dpdo) ligands to form a plane. Two terminal dpdo ligands on Ho(1) shown in **Figure 4.1** are toward one side of the rhombus, with the symmetry-related pair positioned on the other side. Each pair of terminal dpdo ligands positioned on one side forms hydrogen bonds with one water molecule, completing the octahedral-like cavity which could contain Keggin-type polyanions, just like those polyoxometalate anions in NENU-11 previously discussed. These cages are further bridged by dpdo ligands on Ho(2) to form a one-dimensional extended structure. The metal nodes comprised of single metal ions are more accessible than those with bulky metal-oxo clusters. There are labile water ligands on the Ho(III) metal nodes that could leave to facilitate the absorption of Bis(4-nitrophenyl) phosphate (BNPP) nerve agent simulant. Also, the Keggin polyanions serve as counteranions to enhance the Lewis acidity of Ho(III) active sites.

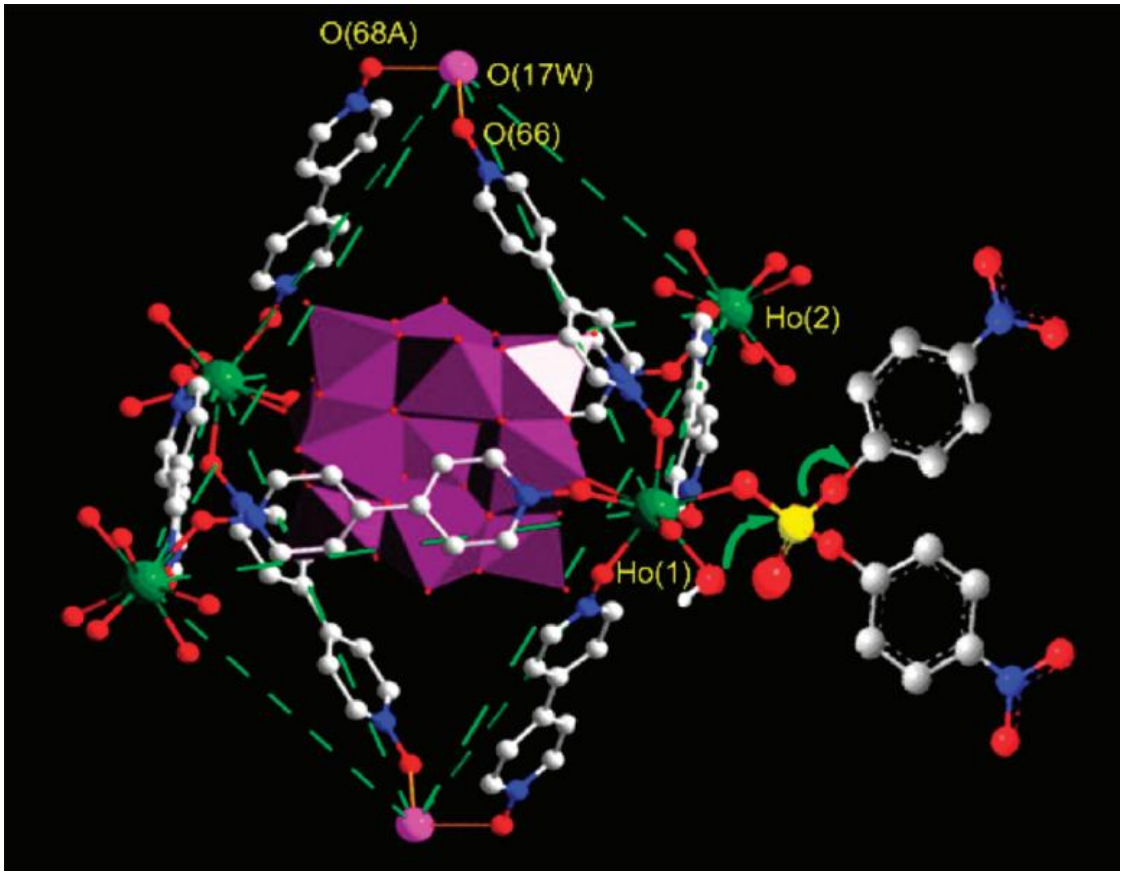

Figure 4.1 Structural illustration of Ho-PMOF. Color code: O (red and pink); Ho (green and yellow); C (gray); N (blue); Keggin-type polyanion (purple). Adapted from **Figure 2** of reference [65]. Adapted with permission. Copyright © 2010, American Chemical Society.

The reaction pathway of BNPP hydrolysis was monitored by UV-vis absorption spectra. Cleavage of BNPP was evidenced by the increase in absorbance at 400 nm due to the formation of an 4-nitrophenoxide anion hydrolysis product. The half-life for the hydrolysis in Ho-PMOF was approximately 3.41 days, relatively long from the current perspective. It should also be noted that the optimum rate was observed in BNPP hydrolysis when pH=4, an acidic environment that deviates from the commonly adopted basic buffer conditions at around pH=10. Among other things, the Ho-PMOF was a proof-of-concept MOF showing promises in nerve agent hydrolysis, a pioneer that opens up a new topic for MOF applications.

Preprints (www.preprints.org) | NOT PEER-REVIEWED | Posted: 14 October 2022 doi:10.20944/preprints202210.0212.v1

4-2. NH_2-MIL-53(Al)

NH2-MIL-53(Al) (where MIL stands for Material Institut de Lavoisier), a derivative of MIL-53 which has amino functionality on its BDC ligands, was first reported in 2012 to be able to hydrolyze DFP--a simulant for the actual nerve agent Sarin (GB) [66] . Bromberg et al were the first who managed to coat MOFs onto a certain substrate for nerve agent simulant hydrolysis. MIL-53 consists of chain-shaped SBUs made up of corner-sharing $AlO_4(OH)_2$ octahedra, and BDC linkers [67] . The shape of the pores in MIL-53 are rhombic 1-D extended channels. Guest molecules in these tunnels are granted direct access to the Al(III) Lewis acidic sites. Moreover, MIL-53 has a unique 'breathing' behavior, which allows its tunnels either to narrow or to narrow its cross-sectional area [68] . At room-temperature, MIL-53 reversibly absorbs water molecules, whose hydrogen bonding with the BDC ligands causes a shrinkage of the pores; while at elevated temperatures, MIL-53 is dehydrated and its pores are expanded. This signifies that the pore size parameters of MIL-53 could flexibly be adjusted by temperature changes for nerve agent simulants of manifold morphologies to fit into the channels.

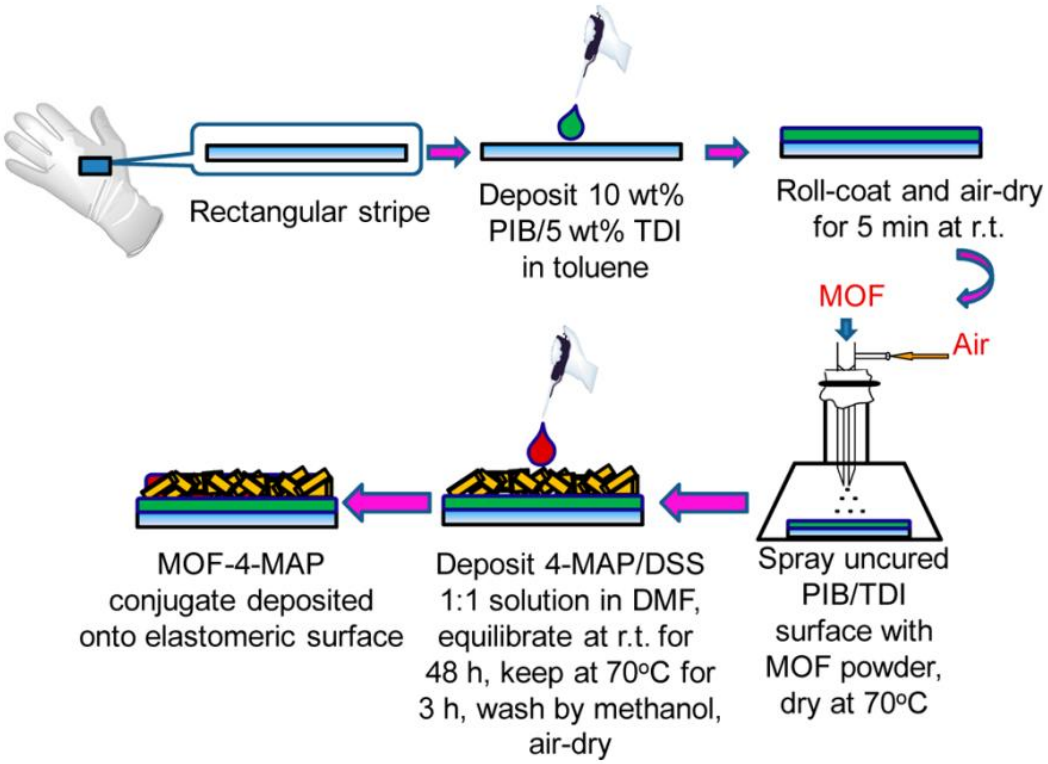

Figure 4.2 Schematic illustration of the synthesis of elastomeric films deposited onto the outer surfaces of the Guardian butyl rubber gloves (Guardian Manufacturing Company, Willard, OH) modified with NH_2-MIL-53/NH_2-MIL-101 that are further functionalized by a strong nucleophile. Adapted from **Figure 6** of reference[66]. Adapted with permission. Copyright © 2012, American Chemical Society.

As shown in **Figure 4.2**, Bromberg et al first deposited a layer of reactive adhesive onto the

Preprints (www.preprints.org) | NOT PEER-REVIEWED | Posted: 14 October 2022 doi:10.20944/preprints202210.0212.v1

surface of the glove. Further spraying of NH_2-MIL-53(Al) onto the reactive adhesives allows the MOF particles to covalently attach to the glove's surface. However, pristine NH_2-MIL-53 manifested little catalytic activity toward DFP hydrolysis. The post-synthetic modification of NH_2-MIL-53 by a strong nucleophile, 4-methylaminopyridine (4-MAP), led to a half-life for DFP hydrolysis of 9 hours. This is because the DFP exposed to the MOF layer started degrading rapidly with the 4-MAP moieties available in the immediate proximity. This research also brings up the possibility of incorporating MOFs into personal protection gears, in order to move these materials from lab to fab to serve practical purposes.

4-3. MIL-101 Family

The MIL-101 family is probably among the most famous trivalent MOFs, including Fe, Al, and Cr. This series of MOFs are constructed from trivalent metal clusters as SBUs and BDC as ligands. But before we discuss the applications of MIL-101 in nerve agent hydrolysis, it is important to realize its difference between MIL-53, a MOF also built from trivalent metal SBUs and BDC linkers. MIL-101 and MIL-53 have distinct structural parameters. As shown in **Figure 4.3**, an SBU in MIL-101 consists of three metal ions bridged by oxygen atoms. Four SBUs of this kind are linked by six NH_2-BDC ligands to form a tetrahedral building block, namely the 'tertiary building unit' or the TBU, which further interconnects with other TBUs in a vex-sharing manner to construct an extended structure of the mtn topology [69] . While the SBUs in MIL-53 are themselves extended rod structures interconnected by terephthalic acid ligands, giving rise to channel-shaped pores which could 'breathe' and fine-tune the pore sizes. MIL-53 is usually considered the thermodynamic product that is structurally more rigid and stabler, MIL-101 its kinetic counterpart which forms faster when mixing the metal precursor and organic ligands (essentially the difference between finishing the assignments in 10 days, and in 10 minutes)[70]. Both MIL-101 and MIL-53 have been shown to hold promise in hydrolyzing the nerve agents and their simulants, and we hereby focus on the hefty amount of research that has been dedicated towards MIL-101 in nerve agent hydrolysis.

Preprints (www.preprints.org) | NOT PEER-REVIEWED | Posted: 14 October 2022 doi:10.20944/preprints202210.0212.v1

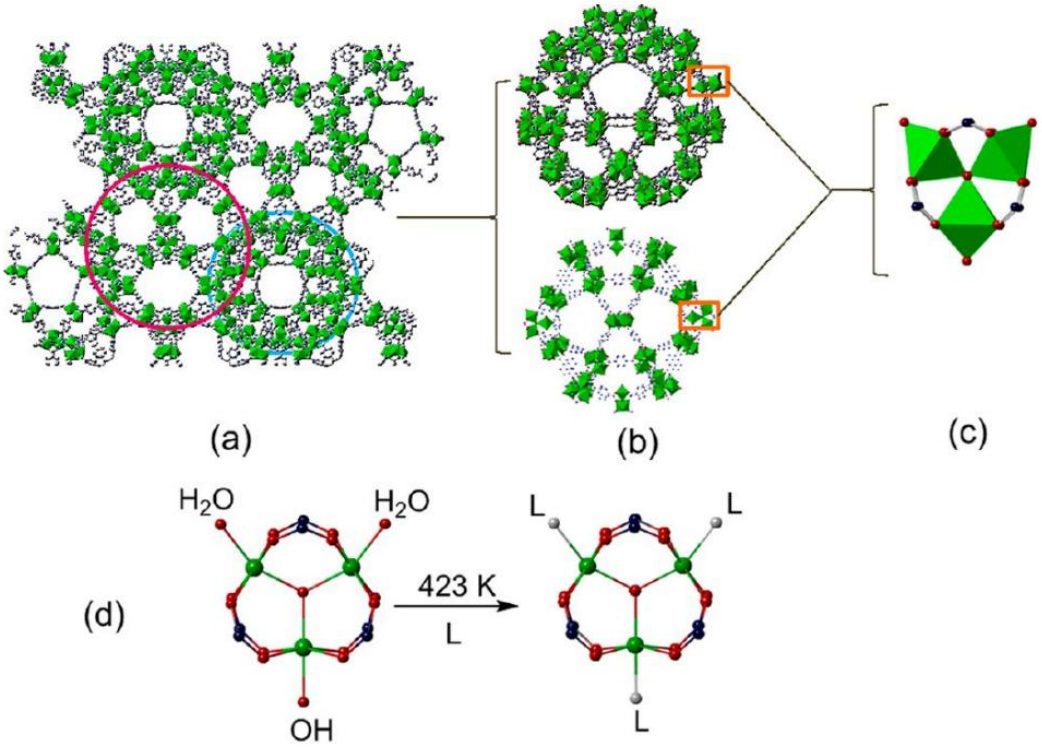

Figure 4.3 Structural illustration of **(a)** MIL-101 of the mtn topology; **(b)** two types of cages formed by linking TBUs in MIL-101; **(c)** an SBU of MIL-101; **(d)** replacement of labile water ligand on an SBU of MIL-101. Adapted from **Figure 1** of reference[71]. Adapted with permission. Copyright © 2013, American Chemical Society.

4-3-1. NH_2-MIL-101(Al)

NH_2-MIL-101(Al) was reported in the same 2012 research paper by Bromberg et al to be able to hydrolyze the nerve agent simulant DFP as its MIL-53 counterpart[66]. With diameters of 29 and 34 Å and pore openings of 12 and 16 Å, the cages in MIL-101 greatly reduce the diffusion barrier for DFP molecules and promote the accessibility of the Al(III) Lewis acidic sites. The half-life for DFP hydrolysis catalyzed by 4-MAP-functionalized NH_2-MIL-101(Al) could be lowered to 0.65 hours, which is a further order of magnitude of improvement compared with NH_2-MIL-53. Recycling experiments for NH_2-MIL-101(Al) particles demonstrated that this material was sufficiently stable over three cycles of the hydrolysis reaction, and, within the experimental error, yielded repeatable, catalytic hydrolysis of DFP.

4-3-2. MIL-101(Cr)

In 2013, the same group probed into the catalytic hydrolysis of paraoxon (DMNP) by MIL-101(Cr) built from unfunctionalized BDC ligands [71]. It is probably intuitive that pristine MIL-101(Cr) exhibits poor catalytic performance in DMNP hydrolysis. However, the labile water terminal ligands as shown in **Figure 4.3** could be easily removed to render coordinatively-unsaturated Cr(III) sites, which could form complexes with a new ligand dialkylaminopyridines (DAAP), a strong nucleophile labeled 'L'. The high hydrolysis reaction turnover was realized by

Preprints (www.preprints.org) | NOT PEER-REVIEWED | Posted: 14 October 2022 doi:10.20944/preprints202210.0212.v1

simultaneous action of the Lewis acid Cr(III) center of the MOF as well as the electron-rich nucleophile, DAAP. This study also illustrated the impact of pH, catalyst loading and the identity of the ligand 'L'. Ceteris Paribus, the rate of DMNP hydrolysis shows a positive correlation with pH value and catalyst loading, and is optimized at pH=10.0 and 10 mg/mL catalyst loading with a half-life of 2.6 hours. Furthermore, as the nucleophilicity of the ligand 'L' increases, the hydrolysis rate also increases due to enhanced local Lewis basicity.

4-3-3. MUV-101(Fe)

Precisely controlling metal node distribution at an atomic level is crucial to span the interest of heterometallic (or multivariate) MOFs to a broad scope of chemical reactions[72]–[74]. The metal ions on the SBUs could be replaced by other metal ions of similar sizes and coordination modes. With a little help from their dopant friends, MOFs could be endowed with better catalytic activities due to the synergistic effect. Castells-Gil et al replaced one Fe(III) ion with a Ti(IV) ion in an SBU of MIL-101(Fe) using post-synthetic modification [53] . The resultant heterometallic MUV-101(Fe) demonstrated outstanding catalytic activity for the hydrolysis of DIFP, a simulant for nerve agent Sarin. The half-life of DIFP hydrolysis using MUV-101(Fe) is around 3 hours. It is worth noting that unlike previous experiments in basic amine solutions, the hydrolysis reactions in this work are carried out free from a basic buffer, providing a non-buffered alternative pathway that has promises in personal protection gears. It is also worth noting in **Figure 4.4** that when the original metal ion in the MIL-101 template, Fe(III), is changed to other metal ions such as Ni(II) or Co(III), the catalytic activity plummets. The pre-eminent activity of MUV-101(Fe) is due to synergetic cooperation of Ti(IV) Lewis acid and Fe(III)--OH Brönsted base sites for a cooperative mechanism that mimics bimetallic purple acid phosphatase (PAP) enzymes in nature. Ti(IV) ions provide Lewis acidic active sites, while Fe(III)--OH moieties constitute a local Bronsted basic environment necessary for the hydrolysis reaction. The example of MUV-101(Fe) offers an outstanding example of synergistic cooperation which involves the 'collaboration' of two metal ions to control the local environment, allowing faster hydrolysis kinetics.

Preprints (www.preprints.org) | NOT PEER-REVIEWED | Posted: 14 October 2022 doi:10.20944/preprints202210.0212.v1

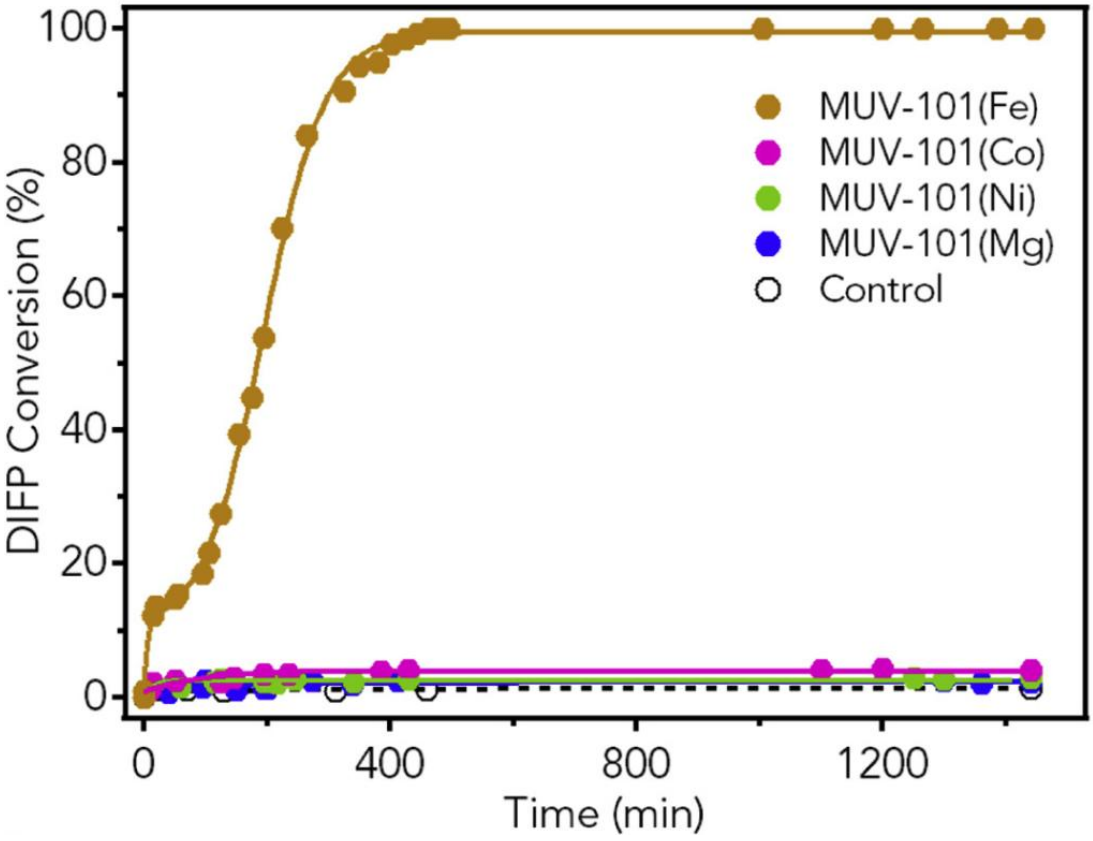

Figure 4.4 DIFP hydrolysis by bimetallic MUV-101(M), where M is Fe, Co, Ni or Mg. Apart from MUV-101(Fe), all others demonstrate poor catalytic turnover. Adapted from **Figure 4 (B)** of reference[53]. Adapted with permission. © 2020 Elsevier Inc.

4-3-4. Magnetic graphene oxide@MIL-101(Fe)

The Fenton reaction allows organophosphorus esters to be directly oxidized to carbon dioxide and water [75] . The photo-Fenton system comprises a catalyst (Fe^{2+}/Fe^{3+}) and an electron scavenger agent (H_2O_2) that can produce hydroxyl radicals with high oxidation power [76] . In a study published by Fakhri et al, a core-shell magnetic support containing magnetic Fe_3O_4 nanoparticles core wrapped by graphene oxide (AFG) shells was used to support MIL-101(Fe) nanoparticles and employed for the oxidation of organophosphorus ester diazonon (DIZ) as shown in **Figure 4.5**[77]. The Fe(III) ions in MIL-101 serve as electron scavengers, consuming electrons and fostering the formation of hydroxyl radicals. The charge transfer efficiency MIL-101(Fe) is further promoted by AFG, as it inhibits the electron-hole recombination efficiency at the Fe sites. What distinguishes this oxidation reaction from a typical nerve hydrolysis reaction is that the Fenton pathway directly decomposes the DIZ into non-hazardous inorganic products. Although the first-order reaction kinetics do not apply to this free radical oxidation (so the half-life value is not constant and could not be determined), the AFG@MIL-101(Fe) could achieve 100% efficiency of DIZ degradation under UV-radiation. Whereas not a hydrolysis reaction, the Fenton pathway derived from Fe(III) ions on MIL-101 offers an alternative approach capable of completely degrading organophosphorus esters into inorganic products not harmful at all to the human body.

Preprints (www.preprints.org) | NOT PEER-REVIEWED | Posted: 14 October 2022 doi:10.20944/preprints202210.0212.v1

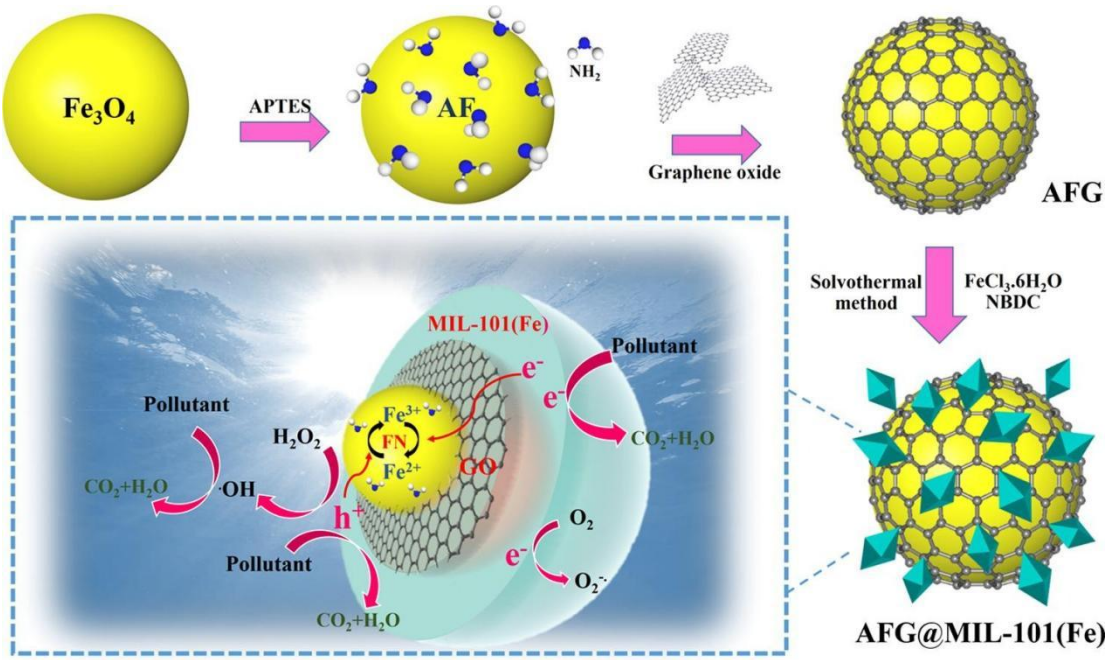

Figure 4.5 Assembly of AFG@MIL-101(Fe) for DIZ degradation. Adapted from the graphical abstract of reference [77] . Adapted with permission. © 2020 International Solar Energy Society. Published by Elsevier Ltd. All rights reserved.

4-3-5. MIL-101(Cr)LZn

We have discussed that there are labile water ligands on the SBUs of MIL-101, which could be removed to form coordinatively unsaturated metal sites. Zhang and his colleagues prepared MIL-101(Cr)LZn catalyst by incorporating polypyridine Zn(II) complexes into the nodes of MIL-101(Cr) by post-synthetic modification [78] . The half-life of the catalytic hydrolysis of DENP could be lowered to 4.5 hours, a significant reduction compared with that catalyzed by pristine MIL-101(Cr), which is 5.9 hours. The remarkable catalytic activity can be ascribed to the implanted functional Zn(II) complexes as Lewis base sites and Cr(III) clusters as Lewis acid sites, an example of the synergistic cooperation in heterometallic MOF.

5. Tetravalent MOFs

Due to the poor reversibility of the strong M(IV)-O bonds formation in the synthesis of tetravalent MOFs, these MOFs require harsh conditions to be obtained in their highly-crystalline form [79] . On the other hand, the strong M-O bonds entail these MOFs great stability in water in a wide range of pH values [80] . The most common tetravalent MOFs are the Zr-based MOFs. The most common SBU in Zr-MOFs, as shown in **Figure 5.1 (A)**, comprises of six Zr(IV) ions bridged by hydroxyl and oxygen ligands [43] . By varying the number of bridging hydroxyl ligands and terminal water molecules, the connectivity of the SBU could be fine-tuned from 4 to 12, which bestows diverse structural parameters upon Zr-MOFs. **Figure 5.1 (B)** shows the formation of a

Preprints (www.preprints.org) | NOT PEER-REVIEWED | Posted: 14 October 2022 doi:10.20944/preprints202210.0212.v1

Schottky defect in Zr-MOFs by ligand substitution, which generates exposed Lewis acidic Zr(IV) sites[81], and could foster the catalytic hydrolysis of nerve agents. Decreasing the connectivity of SBUs, as shown in **Figure 5.1 (C)**, also makes the Zr(IV) more accessible to the nerve agent substrates. Last but not the least, increasing pore volumes could lower the diffusion barriers of large nerve agent molecules, paving their way for reaching Zr(IV) active sites located at the center of Zr-MOF particles, and promoting more efficient hydrolysis reaction. We will be discussing the hydrolysis of nerve agents and their simulants catalyzed by all Zr-MOFs shown in **Figure 5.1**, including UiO-66/67, NU-160X, NU-1000/901, MOF-808 and the recently developed NU-1400 and MIP-212.

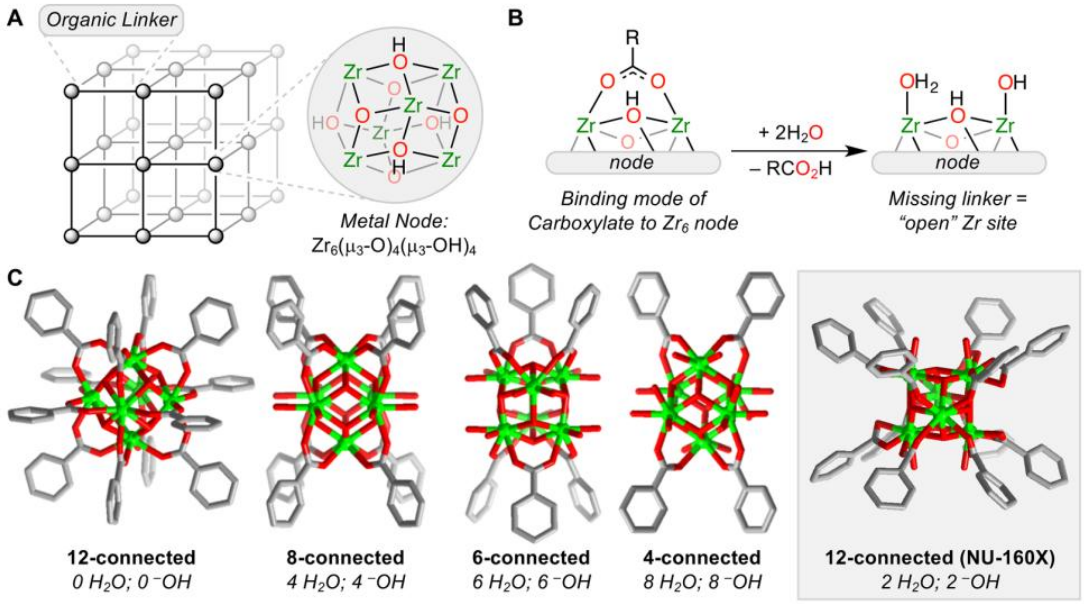

Figure 5.1 (A) The SBU of most of the Zr-MOFs. **(B)** Schottky defects induced by a missing ligand. **(C)** Different possible connectivities of SBUs in Zr-MOFs. Adapted from **Figure 2** of reference[43]. Adapted with permission. Copyright © 2020, American Chemical Society.

5-1. UiO-66

UiO-66 (where UiO stands for the University of Oslo) is probably amongst the most well-known Zr-MOFs, constructed of zirconium-oxo clusters and BDC ligands[58]. The SBU of UiO-66 is a $[Zr_6O_4(OH)_4]$ cluster that contains several Zr-OH-Zr bonds, reminiscent of the bimetallic Zn-OH-Zn active site in phosphotriesterase enzymes in nature as illustrated in **Figure 5.2 (a)** and **(b)**[82]. Inspired by the excellent activity of UiO-66 in phosphate ester methanolysis, this material was employed in the catalytic hydrolysis of DMNP. As shown in **Figure 5.2 (c)**, under room-temperature, the half-life value of DMNP hydrolysis catalyzed by UiO-66 is 45 minutes, which could further decrease to 17 mins by optimization of reaction conditions[83]. This figure falls to 10 mins as the temperature rises to 333 K. UiO-66 afforded a significantly shorter reaction half-life when compared to the Cr-MIL-101 in the presence of DMNP. For the detoxification of real

Preprints (www.preprints.org) | NOT PEER-REVIEWED | Posted: 14 October 2022 doi:10.20944/preprints202210.0212.v1

nerve agents, UiO-66 can hydrolyze GB with a half-life of only 2 minutes, while it has a longer half-life of 31 minutes for GD hydrolysis [83]. This is probably due to the larger alkyl group on GD than that on GB, which could result in more steric hindrance and a larger diffusion barrier. UiO-66 is particularly attractive as a solid catalyst because: (1) it is readily synthesized in high yield and relatively low cost; (2) it is among the most chemically, hydrothermally, and mechanically stable MOFs known. It especially has ultrahigh tolerance to water; and (3) specific functionalities such as $-NH_2$ and $-(OH)_2$ are easily introduced to its pores by synthesizing isoreticular UiO-66 series from differently-functionalized BDC ligands[84].

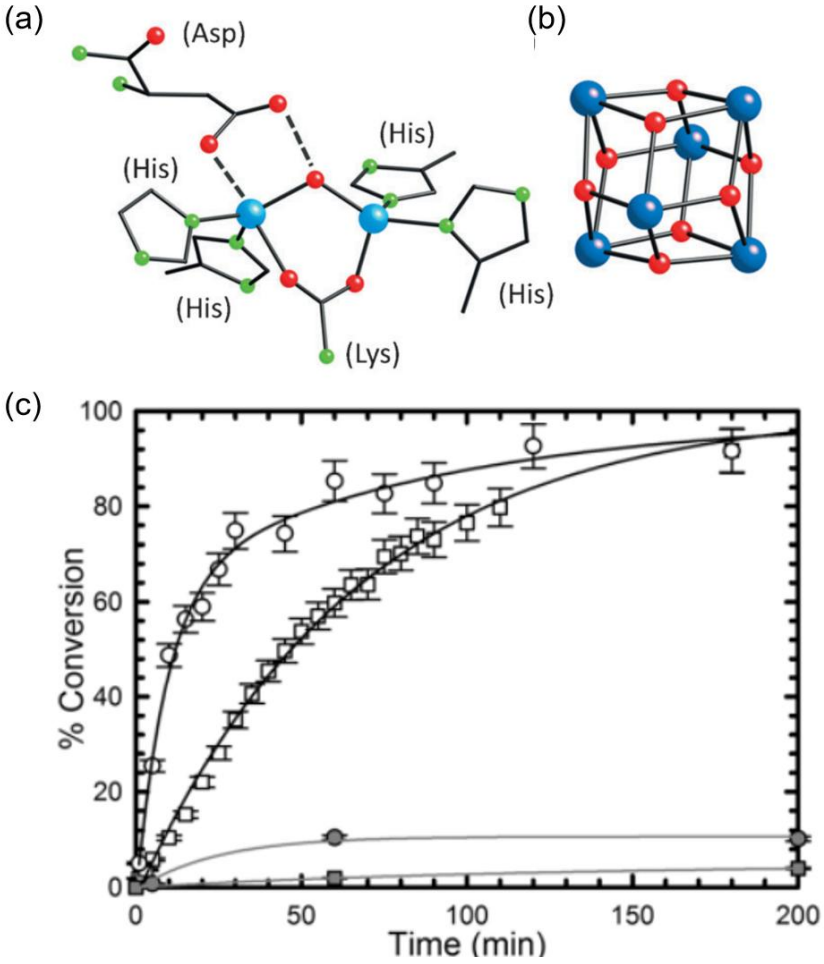

Figure 5.2 (a) A schematic drawing of the structure of the active site of phosphotriesterase. **(b)** The 3D structure of UiO-66. **(c)** Conversion profiles for the hydrolysis of methyl paraoxon in the presence of UiO-66 at room temperature (white squares) and 333 K (white circles) as a function of time. Gray squares and circles represent the conversion profiles for the uncatalyzed reaction at room temperature and 333 K, respectively. Adapted from **Figure 1** and **Figure 3** of reference[82]. Adapted with permission. Copyright © 2014 WILEY - VCH Verlag GmbH & Co. KGaA, Weinheim

Then what are the effects of ligand functionalities on the hydrolysis rate? Contrary to commonsense, the introduction of -OH and $-NO_2$ groups decreases the hydrolysis reaction with half-lives of 60 mins and 45 mins in due order. In contrast, the amino-functionalized UiO-66 showed a tremendously increased with a 30-fold decrease in half-life of only about 1 minute[85].

Preprints (www.preprints.org) | NOT PEER-REVIEWED | Posted: 14 October 2022 doi:10.20944/preprints202210.0212.v1

However, the half-life for the hydrolysis of larger DENP is 35 minutes, which further demonstrates the role that steric effects and diffusion barriers play in microporous MOFs [86] . UiO-66-NH_2 is also capable of gradually hydrolyzing DMNP even in an unbuffered water solution—something that the superior hydrolysis catalyst MOF-808 cannot even achieve. Moreover, UiO-66-NH_2 achieves nearly instantaneous hydrolysis of real nerve agents GA and GD, with half-lives of less than a minute for both[86]. It is hypothesized that the amino moieties serve as a Bronsted base to accelerate the hydrolysis, creating a local basic environment by providing a platform for proton transfer[83]. This is because the nitrogen atom on an amino group adopts the hybridization mode somewhere 'between' sp2 and sp3, leaving its lone-pair not fully in conjugation with the benzene ring and available for proton acceptance [87] . This local Bronsted basic environment is deemed to be a determining factor in the hydrolysis reactions.

5-2. UiO-67

Despite its promises, the pore size in UiO-66 is at best limited. The short BDC ligands constitute two kinds of small pores in UiO-66: tetrahedral ones and octahedral ones. Small pore size may entail a greater diffusion barrier of nerve agent molecules, making them harder to access the active sites located in the interior of MOF particles. Elongation of the BDC ligands by the addition of a benzene ring turns them into BPDC ligands--which further connect with zirconium SBUs to form UiO-67. The relationship between UiO-66 and UiO-67 is coined by Reticular Chemistry to be 'Isoreticular': UiO-66 and UiO-67 have the same Fm-3m space group and fcu topology but are distinct in their lattice parameters[88]. From a macroscopic perspective, UiO-67 is like the 'dilated' UiO-66. The pores in UiO-67 are also larger than those in UiO-66, preventing steric crowding of nerve agent (simulant) molecules at the Zr(IV) active sites. Pristine UiO-67 is able to shorten the half-life of DMNP hydrolysis to 4.5 minutes at 6 mol% catalyst loading [85] . This is nearly a 9-fold rate increase compared with UiO-66. Furthermore, the introduction of an amino group (UiO-67-NH_2) or N,N-dimethylamino group (UiO-67-NMe_2) to the meta position of the BPDC linker only results in only a modest rate enhancement for DMNP hydrolysis compared to that of the pristine UiO-67: UiO-67-NH_2 and UiO-67-NMe_2 both exhibit half-lives of 2 min [85], [89]. UiO-67-NH_2 exhibits a slightly faster hydrolysis rate, probably because the hyper-conjugation between the methyl groups and nitrogen atoms in UiO-67-NMe_2 increases the electron density on nitrogen atoms and slows down the protons from leaving them. Notably, the improvement in catalytic performance is more significant when the amino group is directed towards the node, such as in the case of UiO-66-NH_2, rather than in the meta position when it is pointing away from the node, as it does in UiO-67-NH_2 [89] . This is probably because when the amino groups are directed towards the zirconium nodes, they are able to generate a basic environment around the active sites where nerve agent (simulant) molecules gather.

The UiO-67 family is also promising for the hydrolysis of VX, a real nerve agent. In the degredation of VX, the cleavage of the P-S bond is desired, because hydrolysis of the P−O bond produces the toxic EA-2192. UiO-67-$N(Me)_2$ can selectively hydrolyze the P-S bond of VX in a pH=10 buffered solution with only a half-life of 1.8 mins, unfolding greater efficiency than other previously reported abiotic materials[90].

Preprints (www.preprints.org) | NOT PEER-REVIEWED | Posted: 14 October 2022 doi:10.20944/preprints202210.0212.v1

5-3. MIP-202

MIP-202 (MIP, stands for the materials of the Institute of Porous Materials from Paris), just like UiO-66 family, consists of 12-connected Zr_6 nodes and bidentate linear (offset) aspartic acid ligands. It adopts an fcu topology just like that in UiO-66 [91] . It also bears high crystallinity, along with superior pH resiliency, chemical resistance, and hydrolytic stability comparable to the UiO-66 family [92] . Moreover, the α-amino acid linker aspartic acid is biocompatible and commercially available at large scales, making MIP-202 biomimetic and scalable. MIP-202 demonstrates a half-life of about 30 minutes in the catalytic hydrolysis of DFP and 79.42% conversion rate after 180 mins, which is superior to UiO-66-NH_2 [93]. The better performance of MIP-202 in DFP hydrolysis compared with UiO-66-NH_2 is attributed to the smaller pore opening of MIP-202 (4 Å) than that of UiO-66-NH_2 (5 Å), which allows the easy evacuation of the hydrolysis product DIPP from the pores of MIP-202. In the latter, DIPP molecules may be more stable to just stay in the pores, occupying the Zr sites by Coulomb interaction and finally resulting in irreversible catalytic poisoning.

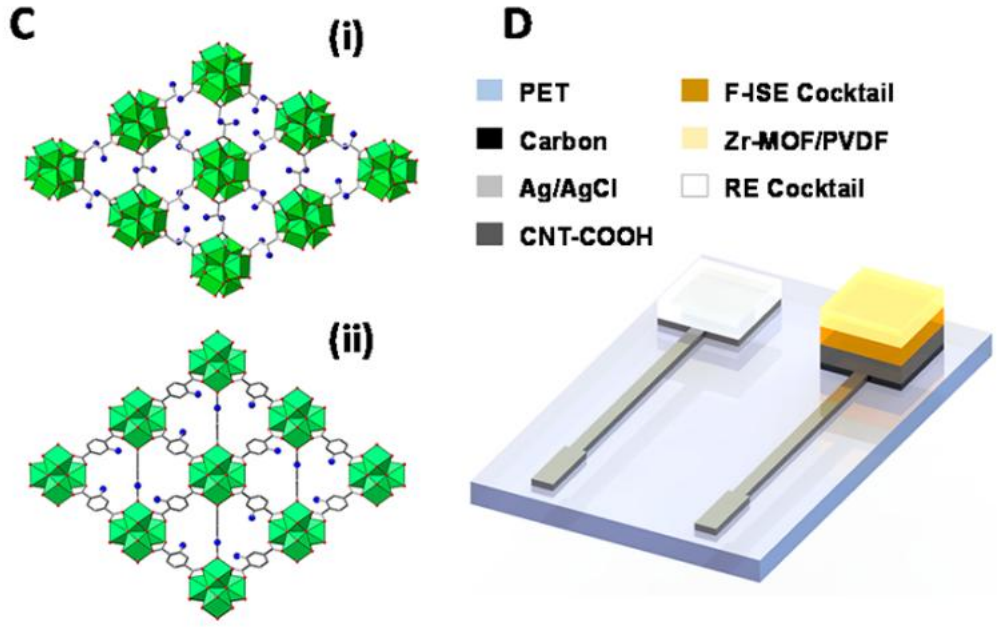

Figure 5.3 (C) Structures of two 12-connected Zr-MOF-based NA degradation catalysts: **(i)** MIP-202(Zr) and **(ii)** UiO-66-NH2, displaying their structural and chemical similarities (Color code: red, oxygen; blue, nitrogen; black, ditopic carboxylated linker; green polyhedra, SBU). **(D)** Composition of the Zr-MOF/F-ISE catalytic sensor chip coupling the degradation and potentiometric detection of F-containing G-type NAs (left electrode, reference electrode (RE); right electrode, working ion-selective electrode (WE)). Copyright © 2021, American Chemical Society.

Considering its outstanding biocompatibility, stability and catalytic activity, a MIP-202-based layer was coupled with a disposable solid-contact fluoride ion-selective electrode (F-ISE) transducer to obtain a MIP-202/F-ISE catalytic electrochemical sensor chip for the detection of F-

Preprints (www.preprints.org) | NOT PEER-REVIEWED | Posted: 14 October 2022 doi:10.20944/preprints202210.0212.v1

containing G-type nerve agents as shown in **Figure 5.3 (B)** [94] . The resulting Zr-MOF-based potentiometric sensor strip represents an attractive alternative to previously reported organophosphorus acid anhydrolase/fluoride (OPAA/F-ISE) and organophosphorus hydrolase/fluoride (OPH/F-ISE) enzymatic biosensors, which are thermally fragile. The MIP-202 biomimetic sensor offers attractive analytical performance along with remarkable storage stability at elevated temperatures over extended durations, including storage conditions of 60 ° C over 30 days. Moreover, the MIP-202/F-ISE sensor chip could operate at near-neutral pH conditions (pH=7.2), signifying its applicability in a realistic situation. Furthermore, to explore the potential of MIP-202/F-ISE in field-detection of nerve agents, a spandex textile-based wearable MIP-202/F-ISE sensor was fabricated, which allowed the detection of DFP aerosols from DFP solution concentrations down to 10 mM. The wearable device manifests great potential for those in first contact with the G-type nerve agents (like warfighters and firefighters) toward the real-time field detection and degradation of airborne G-type nerve agents in low concentrations. Overall, the remarkable thermal and long-term storage stabilities, chemical resistance, pH resiliency, scalability, and biocompatibility, along with the green and low-cost production of MIP-202 may enable the manufacture of sensitive, durable, and low-cost all-weather devices for on-site NA degradation, on-body wearable NA detection and detoxification, and remote field detection of NA threats.

5-4. NU-160X series

Modern knowledge in Reticular Chemistry prompts the synthesis of well-defined NU-160X series (where X=0, 1 or 2)[95]. The 12-connected zirconium SBUs in NU-160X, unlike those in UiO-66, adopt hexagonal-prismatic topology which endows them distinct catalytic properties[96]. Also, by employing a trigonal-prismatic series of peripherally extended triptycene-based linkers as demonstrated in **Figure 5.4 (A)** and **(B)**, H_6PET-X (X = 0, 1, 2), pore sizes in NU-160X could be tuned from microporous to mesoporous (12−27 Å). As shown in **Figure 5.4 (C)** and **(D)**, the NU-160X series exhibit half-lives for DMNP hydrolysis ranging from 1 to 3 minutes under the presence of either liquid N-ethylmorpholine or solid linear PEI. Moreover, NU-1600 together with linear PEI is able to hydrolyze the real nerve agent GD with a half-life of 12 minutes. The improved catalytic activity of NU-160X compared to UiO-66, their 12-connected counterpart, is partially ascribed to the increase in pore apertures. Furthermore, single-crystal X-ray diffraction confirmed the existence of missing linker Schottky defects in NU-160X, which increases the accessibility of the Lewis acidic Zr sites.

Preprints (www.preprints.org) | NOT PEER-REVIEWED | Posted: 14 October 2022 doi:10.20944/preprints202210.0212.v1

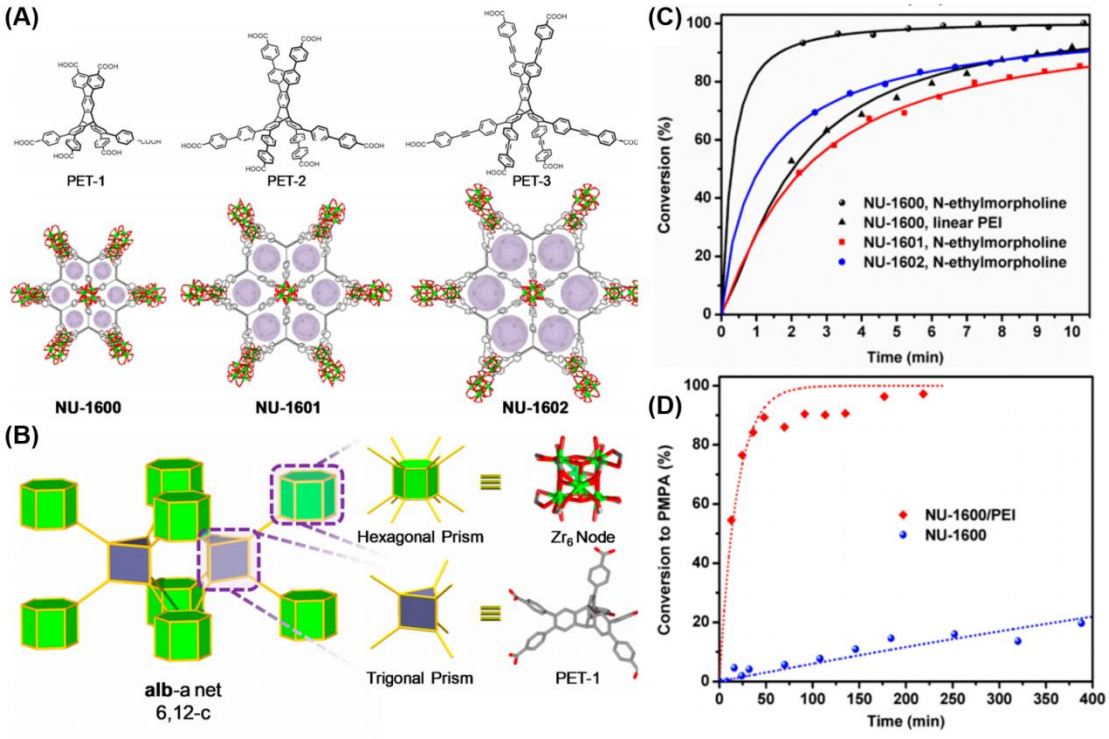

Figure 5.4 (A) Structures of organic ligands in NU-160X. **(B)** The alb-a topology in NU-160X formed by trigonal-prismatic ligands and hexagonal-prismatic SBUs. **(C)** First 10 min of the hydrolysis of DMNP. **(D)** Conversion vs time data for NU-1600/PEI for the hydrolysis of the real nerve agent GD. Adapted from **Figure1**, **Figure 2** and **Figure 3** of reference [96] Adapted with permission. Copyright © 2019, American Chemical Society.

5-5. NU-1000 series, NU-901 and Spriof-MOFs

Increasing the accessibility of Zr nodes can further increase the hydrolysis rate. A problem specifically with these 12-connected SBUs is that they have such high connectivity that the active Zr sites are largely occupied by ligands, and the only approach to increase Zr accessibility is by introducing Schottky defects by removing ligands—which could pose challenges in design and synthesis. Another effective strategy to expose more Zr active sites is to decrease the connectivity of SBUs by replacing linkers with terminal -OH and -OH_2 groups. When there are fewer ligands connected to the SBUs, more Zr active sites could be exposed to nerve agent substrates. NU-1000 is built up from 8-connected (instead of 12-connected) SBUs and tetratopic 1,3,6,8(p-benzoate)pyrene linkers ($TBAPy^{4-}$) [97] , and it shows superior catalytic performance in DMNP hydrolysis compared with UiO-66, with a half-life of 15 minutes[98]. NU-1000 is also capable of hydrolyzing the actual nerve agent GD with a half-life of 36 minutes. DFT calculations reveal that the nerve agent (simulant) molecules are anchored to the 8-connected SBUs by forming hydrogen bonds with the terminal -OH and OH_2 groups, and the hydrogen bonding could further be stabilized by π - π stacking between the benzene rings on DMNP and $TBAPy^{4-}$ linkers. Whereas UiO-66 has too small pores, NU-1000 has mesoporous channels that could be functionalized by $[Mg(OMe)_2(MeOH)_2]_4$, and the resultant composite could achieve unbuffered hydrolysis of real nerve agent VX for a half-life of 10.1 minutes[99].

Preprints (www.preprints.org) | NOT PEER-REVIEWED | Posted: 14 October 2022 doi:10.20944/preprints202210.0212.v1

Computational simulations suggest that in pristine NU-1000, the rate-limiting step in the hydrolysis is the displacement of a terminal $-OH_2$ with the phosphoryl oxygen of the nerve agent (simulant). So to further speed up the hydrolysis reactions, NU-1000 was heated under vacuum to partially remove some terminal water ligands (denoted as NU-1000-dehyd) [100] . The new NU-1000-dehyd material exhibited over 10-fold enhancement in the rate of hydrolysis compared with pristine NU-1000, with a 1.5 minutes and 3 minutes half-life for DMNP and GD hydrolysis. The significant enhancement in hydrolysis rate is attributed to the stronger hydrogen-bonding interaction between DMNP molecules and Zr metal sites. With optimizations in hydrolysis conditions, the half-lives for DENP, GD and VX hydrolysis could further be lowered to 2.6 minutes, less than one minute, and 5.3 minutes in due order, affording even greater promises in real nerve agent hydrolysis.

Reticular Chemistry also allows the synthesis of distinct topology from the same precursors. NU-901 is synthesized from the same metal source and linkers as NU-1000, with 8-connected SBUs and 4-connected ligands but scu (square and cube) topology rather than csq topology in NU-1000 [101], [102] . The rhombic-shaped 1-D channels with catalytically active Zr−O−Zr sites pointing into the channels, as well as the small crystal size of over 300 nm, make NU-901 promising for the catalytic hydrolysis of nerve agent simulants. Under 6 mol% of N-ethylmorpholine, NU-901 catalyzes DMNP hydrolysis with a half-life of over 1 minute--almost instantaneous [103] . Besides N-ethylmorpholine, non-volatile solid bases are also employed. The half-life for the hydrolysis of DMNP in the presence of PAMAM dendrimer and branched PEI was found to be 1.1 and 1.2 min, comparable to the small organic base. For the PANAM dendrimer and branched PEI are larger in molecular weight and are less likely to evaporate than small organic base, these solid bases—combined with the excellent performance of NU-901 and NU-1000 in nerve agent hydrolysis, hold great promises in protective suit applications.

Spriof-MOF, a Zr-based MOF containing 4,4′,4″,4‴-(9,9′-spirobi[fluorene]-2,2′,7,7′-tetrayl)tetrabenzoic acid as ligand, was also synthesized for the catalytic hydrolysis of DMNP [104] . The SBU in Spirof-MOF is a 8 connected $[Zr_6(\mu 3\text{-}O)_8(COOH)_8(H_2O)_8]$. Spirof-MOF has the same 8-connected Zr_6 cluster node as NU-1000, which is an exposed Lewis acidic site for nerve agent hydrolysis. The pyrene unit of NU-1000 was replaced by spirobifluorene, which is similar in size but with a reduced π -conjugation. Despite its small pore size (6 and 8 Å), Spriof-MOF in bulk could hydrolyze DMNP with a half-life of 7.5 minutes—half the value of pristine NU-1000. The possible mechanism is that the closer distance between the adjacent Zr_6 nodes of Spirof-MOF than that of NU-1000 makes the Zr(IV) active sites more readily accessible to DMNP substrate. By decreasing the particle size from 16 μm to 1 μm, the hydrolysis half-life could be optimized to 1.8 mins—comparable to dehydrated NU-1000. Spriof MOF demonstrates the decisive role that MOF particle size could play in nerve agent hydrolysis. Smaller particle size means more Zr-SBUs directly exposed to the surroundings, making the Lewis acidic active sites more readily available for DMNP substrates.

Preprints (www.preprints.org) | NOT PEER-REVIEWED | Posted: 14 October 2022 doi:10.20944/preprints202210.0212.v1

5-6. MOF-808

We have seen that 8-connected NU-1000, NU-901 and Spriof-MOFs give rise to higher reaction rate compared with the 12-connected pristine UiO-66, so what if the connectivity further decreases to 6? Six-connected Zr_6 nodes and 3-connected BTC linkers give rise to MOF-808, which remains one of the most efficient MOF catalysts reported up till date [105]. In activated MOF-808, there are six OH groups and six OH_2 groups on each SBU (which had been already occupied by linkers if the SBU is 12-connected). A greater amount of Zr(IV) active sites are exposed, which affords greater overall catalytic turnover. MOF-808 is also synthesized from cheap and commercially available BTC linkers, making its production easily scalable. Under 6 mol% catalyst loading and aquous N-ethylmorpholine, the half-lives of DMNP and GD hydrolysis catalyzed by MOF-808 is just around 30 s and 2 mins--almost instantaneous [106]. The large pore openings of MOF-808 allows it to be functionalized with $[Mg(OMe)_2(MeOH)_2]_4$, and the resultant composite could hydrolyze VX in an unbuffered water solution with a half-life of less than 2 minutes [99]. MOF-808 is also recently revealed to be a highly efficient and regenerable catalyst for Novichok agent (also known as the A-type nerve agent) hydrolysis under pH=10[107]. The initial degradation rates of Novichok agents **A-230** and **A-232** were instantaneous, with half-lives of less than 30 seconds. In contrast to the V- and G-series of agents we have discussed earlier, the degradation of Novichoks is demonstrated to proceed in two consecutive hydrolysis steps. Initial extremely rapid P–F bond breaking is followed by MOF-catalyzed removal of the amidine group by P–N bond hydrolysis from the intermediate product. This is a pioneering (and the one-and-only) study demonstrating MOFs' potential in the catalytic hydrolysis of Novichok agents, which are relatively novel compared with the traditional G- and V-type nerve agents [108]. This work also reveals a hydrolysis pathway for Novichoks—which has been arguably unclear to researchers.

Then, to further explore its potential in solid-state protective gear applications, MOF-808 was mixed with grounded PEI particles, and was coated to a layer of cotton textile by a facile gel-based dip-coating technique [109]. The resultant MOF-808/PEI/fiber composite was tested for solid-state DMNP and GD hydrolysis, with relative humidity (RH)=50% and no external water source. The half-lives are 24 minutes and 12 minutes respectively. Besides PEI, imidazole molecules serving as non-volatile bases were also incorporated into the pores of MOF-808, and the resultant Im@MOF-808 composite resembles phosphotriesterase's active site as well as its ligated histidine residues [110]. Im@MOF-808 could hydrolyze DMNP with a half-life less than 30 seconds in water solution, and 15 minutes in RH=99% without bulk water. It is worth noting that although MOF-808/PEI/fibre and Im@MOF-808 composites with heterogeneous bases can outperform some previously reported MOFs with homogeneous base in DMNP and GD hydrolysis, they still suffer from sluggish kinetics of nerve agent degradation compared with MOF-808 in a homogeneous base solution. This is because only the surface of the PEI macromolecule particles can interact with the surface of the MOF-808 particles, limiting the amount of Zr(IV) active sites that could catalyze the hydrolysis, leading to a fall in the overall catalytic turnover. To further resolve this decrease in the reaction kinetics, 1,3-butadiene diepoxide as the cross-linking reagent was added to a water solution of branched PEI to obtain a branched PEI hydrogel [111], [112]. Then the branched PEI hydrogel granules, replacing the pristine PEI particles, were mixed with MOF-808, and the resultant mixture was integrated onto cotton fibers by the same dip-coating

Preprints (www.preprints.org) | NOT PEER-REVIEWED | Posted: 14 October 2022 doi:10.20944/preprints202210.0212.v1

technique. Ceteris paribus (RH=50%, catalyst loading=6 mol%), the MOF-808/hydrogel/fiber composite is able to hydrolyze DMNP with a half-life of just 1 minute. This composite also degrades nearly 100% VX after 10 min, and 60% of the GD after 10 minutes--significant improvements compared with previous heterogeneous composites, and even comparable to results obtained in a water solution with a volatile base. The elevated catalytic turnover is attributed to the more sufficient interaction between PEI hydrogel and MOF-808 particles due to larger contact areas brought by hydrogel incorporation, as well as an increase in water concentration near the Zr(IV) active sites. This facile processing method of the MOF-808/hydrogel/fiber composite could be easily scaled up, which could lay a solid foundation for the large-scale production MOF based protective gear, such as protective masks and cloths.

MOF-808 with only zirconium as the Lewis acidic site are capable of efficiently hydrolyzing many nerve agents and simulants; however, in pure unbuffered water solution, MOF-808 exhibits poor catalytic activity in DIFP hydrolysis, with a long half-life of 46.2 minutes. By replacing some Zr(IV) ions on the SBUs with Ce(IV) ions, heterometallic (multivariate) Ce-Zr-MOF-808 could be synthesized with different Ce:Zr ratios [113] . Due to synergistic effects, Ce-Zr-MOF-808 could achieve more rapid unbuffered DIFP hydrolysis with a half-life of 6 minutes. This value could further be lowered to 2 minutes by doping $Mg(OMe)_2$, a third metal site. This example of heterometallic MOF-808 helps illustrate the potential of synergistic effects in assisting nerve agent hydrolysis in multivariate MOFs.

5-7. NU-1400

The connectivity of the metal nodes could even decrease to four--which gives NU-1400 combined with tetratopic triphenyl-based linkers (TPTC)[114]. Such low connectivity endows NU-1400 with guest-dependent structural flexibility as shown in **Figure 5.6**: different guest molecules could result in different pore sizes and unit cell parameters. Guest molecules residing in NU-1400 favor expanded pore sizes and lattice structure, whereas the evacuation of these guest molecules causes a shrinkage of the pore sizes and could lead to a 48% contraction of the pore volume. This structural flexibility plays a vital role in catalytic DMNP hydrolysis: The expanded form of NU-1400 has a half-life (t=3 mins) that is more than 20 times lower than that of its contracted form (t=80 mins). This is because the pore opening in the contracted NU-1400 is smaller than the size of the DMNP molecules, limiting their diffusion through the pores; expanded NU-1400 has larger pore openings and allows DMNP to access more Zr(IV) active sites. Although either contracted or expanded NU-1400 has a better catalytic activity towards DMNP hydrolysis compared with MOF-808. the structural flexibility of NU-1400 illustrates the exciting potential for pore-selective catalysis and may shed light on the design of MOFs with flexible pore sizes for adjustable activity in nerve agent hydrolysis.

Preprints (www.preprints.org) | NOT PEER-REVIEWED | Posted: 14 October 2022 doi:10.20944/preprints202210.0212.v1

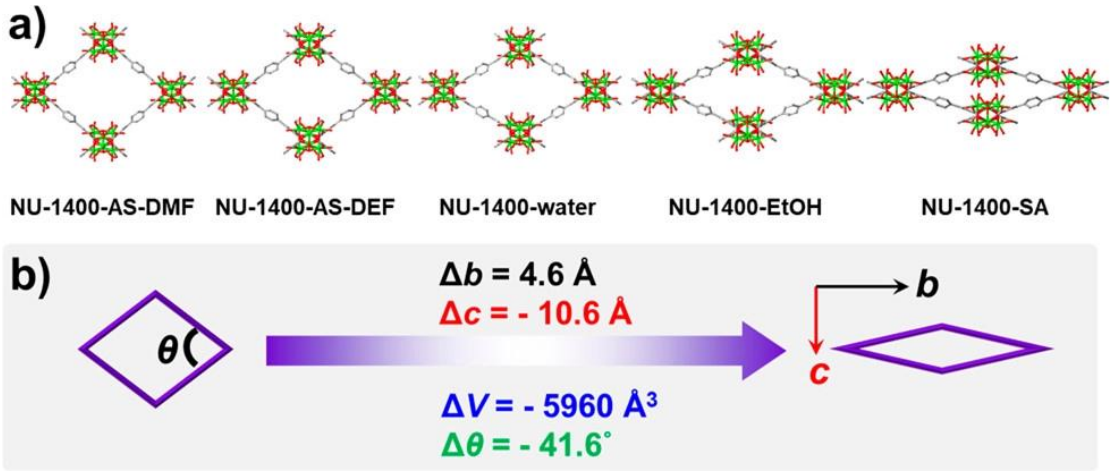

Figure 5.6 Structural changes of NU-1400 in different solvents from single crystal X-ray diffraction data. **(a)** Pore structures of as-synthesized (AS) NU-1400 in DMF, DEF, water, ethanol and no solvent after supercritical CO2 activation (SA) viewed along a axis. **(b)** Schematic representation of the changes of the diamond-shape channel. Adapted from **Figure 3** of reference[114]. Adapted with permission. Copyright © 2018, American Chemical Society.

6. Challenges and Outlook

We have seen a hefty number of examples of MOFs' catalytic hydrolysis of nerve agent simulants and actual nerve agents, and the capability of each MOF has been examined separately to emphasize how differences in MOFs' structures could lead to different nerve agent hydrolysis pathways and outcomes. Some may believe that MOFs are unstable in water and are too expensive to be mass-produced. "Not quite", I argue. MOFs with higher connectivity have demonstrated outstanding stability in water, and some of them including MOF-808 are made from commercially available linkers. There have been reports highlighting the scale-up synthesis of MOFs. Besides, compared with saving more money, saving more lives are undoubtedly more desirable. Nevertheless, there do exist certain remaining challenges that MOFs are to overcome.

The very first to consider is the versatility of a certain MOF catalyst. How many types of nerve agents (simulants) is a MOF able to efficiently hydrolyze? It could be argued that many MOFs are efficient at hydrolyzing only specific nerve agents and suffer from low turnover frequencies and long half-lives when hydrolyzing others. To combine the 'expertise' of different MOFs, hybrid MOF-on-MOF structures are desired. There have been efforts in research that highlight the epitaxial growth and metal/ligand exchange techniques to synthesize manifold hybrid MOF-on-MOF structures--including core-shell, yolk-shell, hollow multi-shell, and layer-on-layer [115] . MOF-on-MOF composites have already shown improved performances in gas adsorption/separation and catalysis compared with the individual MOFs [116], [117], which may shed light on the development of future hybrid MOF-on-MOF catalysts for nerve agent hydrolysis. To go further into versatility, there has been very little research that focuses on MOFs' catalytic hydrolysis of Novichoks, compared with G- and V-type nerve agents. Except MOF-808, no MOFs

Preprints (www.preprints.org) | NOT PEER-REVIEWED | Posted: 14 October 2022 doi:10.20944/preprints202210.0212.v1

have ever been reported to catalytically hydrolyze Novichoks [107] . This could be due to the limited data availability related to these A-type agents, as well as the lack of a nerve agent simulant that mimics the activity of Novichoks and poses less threat to researchers. Nevertheless, the recently reported Novichok attacks have urged the dire need for a detoxification agent against these extremely lethal chemicals. Suppose less toxic simulants of Novichoks were to be utilized. In that case, more research on Novichoks could be carried out under safer conditions, paving the way for the development of more efficient MOF Novichok hydrolysis catalysts.

Another factor worth attention is the relatively limited understanding of the underlying hydrolysis mechanisms in MOFs' pores. The same hydrolysis pathway might just undergo very different mechanisms in divalent, trivalent and tetravalent MOFs, for the participation of different metal ions may favor different kinetics. Even in the most studied tetravalent MOFs, there exist discrepancies about the proposed hydrolysis mechanism. The hydrolysis mechanism also depends on the system's pH, as different mechanisms may have different optimal pH values [64] . If more mechanistic insights on the detoxification process happening in MOFs' pores could be unveiled, more efficient MOF catalysts could be designed in accordance with the underlying hydrolysis mechanisms, fostering more efficient degradation of nerve agents.

The sluggish kinetics of the solid-state hydrolysis system without bulk water compared with the hydrolysis system buffered by basic solution is also worth noting. Almost all MOF catalysts reported by far see a loss in reaction rates and elongation in half-lives. There are mainly 2 causes for this inevitable slowdown. First, as discussed in Section 5-7, because the solid non-volatile bases are in particle/granule form, only the surface of the base particles can interact with the surface of the MOF particles, limiting the amount of Lewis acid active sites that could catalyze the hydrolysis. Second, when the hydrolysis reaction is finished, the product needs to be evacuated from the active metal sites of MOF to free up more space for another undegraded nerve agent molecule to be hydrolyzed at this site. Bulk water could "wash away" the hydrolysis product; while in a solid-state system the product may remain at the metal site, occupying this site and ultimately leading to catalytic poisoning. A potential strategy to enhance local water concentration other than hydrogel incorporation is to utilize MOFs that could harvest water directly from the air (even from desert air with low RH). Prominent examples of MOFs able to capture water from dry air include MOF-801, MOF-303 and MOF-841 [50], [80]. When these MOFs are composited with the catalytically active MOFs like MOF-808, they are expected to absorb water directly from the air and form water clusters in their pores, giving rise to a water 'reservoir' that can assist the effective evacuation of hydrolysis products and the overall catalytic turnover.

Besides the 3 challenges mentioned above, researchers shall bear in mind the importance of metal ion accessibility—the determining factor affecting the hydrolysis rate. In future research, efforts shall be devoted towards making metal active sites more available for nerve agents, but how? There are usually three approaches to increase the accessibility of metal ions on the SBUs. First, increasing pore apertures. The enlargement of pore size decreases the diffusion barriers and allows faster diffusion of nerve agent molecules in and out of the pores. Second, lowering node connectivity and precisely introducing defects on the SBUs. If an SBU binds to fewer linkers, the metal ions on it have greater exposure to the surrounding environment. This is because the original

linkers are replaced by terminal aqua (-OH_2) and hydroxo (-OH) ligands. Third, decreasing the crystallite sizes. Well-defined nanosized MOF (MOFs less than 500 nm as defined by Farha et al) crystals entail better catalytic performances than their bulky counterparts, because in the latter case the nerve agent molecules could not reach the interior of the large MOF crystals due to diffusion barriers, and only those SBUs on the surface layer of these MOF crystals could serve as Lewis acidic centers[118].

The past 11 years have seen a surge of research that has brought pre-eminent advancements to MOFs' catalytic degradation of nerve agents, and has accumulated valuable insights into the future design of even more promising MOF catalysts. Amongst all the challenges, there lies opportunities more than meets the eye. It is just through resolving remaining challenges that scientists today take their leap forward, and endow the community with a better tomorrow than when they found it yesterday.

7. Conflicts of Interest

The author declares no conflicts of interest.

8. Acknowledgments

The author thanks Kaikai Ma at Northwestern University for the helpful discussions, and Wei Gong at Northwestern University for the kind invitation.

9. References

[1] S. Chauhan *et al.*, "Chemical warfare agents," *Environ Toxicol Pharmacol*, vol. 26, no. 2, pp. 113–122, Sep. 2008, doi: 10.1016/j.etap.2008.03.003.

[2] N. H. Johnson, J. C. Larsen, and E. C. Meek, "Historical perspective of chemical warfare agents," *Handbook of Toxicology of Chemical Warfare Agents*, pp. 17–26, Jan. 2020, doi: 10.1016/B978-0-12-819090-6.00002-7.

[3] E. Nepovimova and K. Kuca, "Chemical warfare agent NOVICHOK - mini-review of available data," *Food and Chemical Toxicology*, vol. 121, pp. 343–350, Nov. 2018, doi: 10.1016/J.FCT.2018.09.015.

[4] J. Bajgar, J. Fusek, J. Kassa, K. Kuca, and D. Jun, "Global impact of chemical warfare agents used before and after 1945," *Handbook of Toxicology of Chemical Warfare Agents*, pp. 27–36, Jan. 2020, doi: 10.1016/B978-0-12-819090-6.00003-9.

[5] R. R. N. Alves and R. R. Duarte Barboza, "What About the Unusual Soldiers? Animals Used in War," in *Ethnozoology*, Elsevier, 2018, pp. 323–337. doi: 10.1016/B978-0-12-809913-1.00017-X.

[6] M. Kloske and Z. Witkiewicz, "Novichoks – The A group of organophosphorus chemical warfare agents," *Chemosphere*, vol. 221, pp. 672–682, Apr. 2019, doi: 10.1016/J.CHEMOSPHERE.2019.01.054.

[7] L. Szinicz, "History of chemical and biological warfare agents," *Toxicology*, vol. 214, no. 3, pp. 167–181, Oct. 2005, doi: 10.1016/J.TOX.2005.06.011.

[8] Y.-C. Yang, "Chemical Detoxification of Nerve Agent VX," *Acc Chem Res*, vol. 32, no. 2, pp. 109–115, Feb. 1999, doi: 10.1021/ar970154s.

[9] T. Nakagawa and A. T. Tu, "Murders with VX: Aum Shinrikyo in Japan and the assassination of Kim Jong-Nam in Malaysia," *Forensic Toxicol*, vol. 36, no. 2, pp. 542–544, Jul. 2018, doi: 10.1007/s11419-018-0426-9.

[10] P. R. Chai, B. D. Hayes, T. B. Erickson, and E. W. Boyer, "Novichok agents: a historical, current, and toxicological perspective," *Toxicol Commun*, vol. 2, no. 1, pp. 45–48, 2018.

[11] J. Clancy and A. McVicar, *Handbook of chemical and biological warfare agents*. CRC press, 2007.

[12] J. Bajgar *et al.*, "Changes of acetylcholinesterase activity in different rat brain areas following intoxication with nerve agents: Biochemical and histochemical study," *Chem Biol Interact*, vol. 165, no. 1, pp. 14–21, Jan. 2007, doi: 10.1016/J.CBI.2006.10.006.

[13] V. Aroniadou-Anderjaska, J. P. Apland, T. H. Figueiredo, M. de Araujo Furtado, and M. F. Braga, "Acetylcholinesterase inhibitors (nerve agents) as weapons of mass destruction: History, mechanisms of action, and medical countermeasures," *Neuropharmacology*, vol. 181, p. 108298, Dec. 2020, doi: 10.1016/J.NEUROPHARM.2020.108298.

[14] R. Pita and J. Domingo, "The Use of Chemical Weapons in the Syrian Conflict," *Toxics*, vol. 2, no. 3, pp. 391–402, Jul. 2014, doi: 10.3390/toxics2030391.

[15] P. R. Chai, E. W. Boyer, H. Al-Nahhas, and T. B. Erickson, "Toxic chemical weapons of assassination and warfare: nerve agents VX and sarin," *Toxicol Commun*, vol. 1, no. 1, pp. 21–23, Jan. 2017, doi: 10.1080/24734306.2017.1373503.

[16] J. A. Vale, T. C. Marrs, and R. L. Maynard, "Novichok: a murderous nerve agent attack in the UK," *Clin Toxicol*, vol. 56, no. 11, pp. 1093–1097, 2018.

[17] J. Masterson, "Novichok Used in Russia, OPCW Finds," *Arms Control Today*, vol. 50, no. 9, pp. 25–26, 2020.

[18] P. R. Chai *et al.*, "Wartime toxicology: the spectre of chemical and radiological warfare in Ukraine," *Toxicol Commun*, vol. 6, no. 1, pp. 52–58, Dec. 2022, doi: 10.1080/24734306.2022.2056374.

[19] L. Zhang *et al.*, "Rapid detection of nerve agents in environmental and biological samples using a fluorescent probe," *Spectrochim Acta A Mol Biomol Spectrosc*, vol. 275, p. 121171, Jul. 2022, doi: 10.1016/J.SAA.2022.121171.

[20] L. Jiang, Y. Sun, Y. Chen, and P. Nan, "From DNA to Nerve Agents – The Biomimetic Catalysts for the Hydrolysis of Phosphate Esters," *ChemistrySelect*, vol. 5, no. 30, pp. 9492–9516, Aug. 2020, doi: 10.1002/slct.202001947.

[21] M. J. Field and T. W. Wymore, "Multiscale modeling of nerve agent hydrolysis mechanisms: a tale of two Nobel Prizes," *Phys Scr*, vol. 89, no. 10, p. 108004, Oct. 2014, doi: 10.1088/0031-8949/89/10/108004.

[22] T. A. Hamlin, M. Swart, and F. M. Bickelhaupt, "Nucleophilic Substitution (S_N2): Dependence

 doi:10.20944/preprints202210.0212.v1

on Nucleophile, Leaving Group, Central Atom, Substituents, and Solvent," *ChemPhysChem*, vol. 19, no. 11, pp. 1315–1330, Jun. 2018, doi: 10.1002/cphc.201701363.

[23] Z. Wu, X. Wu, Y. Yang, T. bin Wen, and S. Han, "A rhodamine-deoxylactam based sensor for chromo-fluorogenic detection of nerve agent simulant," *Bioorg Med Chem Lett*, vol. 22, no. 20, pp. 6358–6361, Oct. 2012, doi: 10.1016/J.BMCL.2012.08.077.

[24] Y. C. Yang, J. A. Baker, and J. R. Ward, "Decontamination of chemical warfare agents," *Chem Rev*, vol. 92, no. 8, pp. 1729–1743, Dec. 1992.

[25] B. Picard, I. Chataigner, J. Maddaluno, and J. Legros, "Introduction to chemical warfare agents, relevant simulants and modern neutralisation methods," *Org Biomol Chem*, vol. 17, no. 27, pp. 6528–6537, 2019, doi: 10.1039/C9OB00802K.

[26] J. Nawała, P. Jóźwik, and S. Popiel, "Thermal and catalytic methods used for destruction of chemical warfare agents," *International Journal of Environmental Science and Technology*, vol. 16, no. 7, pp. 3899–3912, Jul. 2019, doi: 10.1007/s13762-019-02370-y.

[27] H. Carlsson, M. Haukka, and E. Nordlander, "Structural and Functional Models of the Active Site of Zinc Phosphotriesterase," *Inorg Chem*, vol. 43, no. 18, pp. 5681–5687, Sep. 2004, doi: 10.1021/ic0354522.

[28] Z. Prokop, F. Opluštil, J. DeFrank, and J. Damborský, "Enzymes fight chemical weapons," *Biotechnol J*, vol. 1, no. 12, pp. 1370–1380, Dec. 2006, doi: 10.1002/biot.200600166.

[29] K.-Y. Wong and J. Gao, "The Reaction Mechanism of Paraoxon Hydrolysis by Phosphotriesterase from Combined QM/MM Simulations," *Biochemistry*, vol. 46, no. 46, pp. 13352–13369, Nov. 2007, doi: 10.1021/bi700460c.

[30] A. N. Bigley and F. M. Raushel, "Catalytic mechanisms for phosphotriesterases," *Biochimica et Biophysica Acta (BBA) - Proteins and Proteomics*, vol. 1834, no. 1, pp. 443–453, Jan. 2013, doi: 10.1016/J.BBAPAP.2012.04.004.

[31] F. C. G. Hoskin and A. H. Roush, "Hydrolysis of Nerve Gas by Squid-Type Diisopropyl Phosphorofluoridate Hydrolyzing Enzyme on Agarose Resin," *Science (1979)*, vol. 215, no. 4537, pp. 1255–1257, Mar. 1982, doi: 10.1126/science.7058344.

[32] O. M. Yaghi, M. J. Kalmutzki, and C. S. Diercks, *Introduction to reticular chemistry: metal-organic frameworks and covalent organic frameworks*. John Wiley & Sons, 2019.

[33] H. Li, M. Eddaoudi, M. O'Keeffe, and O. M. Yaghi, "Design and synthesis of an exceptionally stable and highly porous metal-organic framework," *Nature*, vol. 402, no. 6759, pp. 276–279, 1999.

[34] H.-C. "Joe" Zhou and S. Kitagawa, "Metal–Organic Frameworks (MOFs)," *Chem. Soc. Rev.*, vol. 43, no. 16, pp. 5415–5418, Jul. 2014, doi: 10.1039/C4CS90059F.

[35] H. Furukawa, K. E. Cordova, M. O'Keeffe, and O. M. Yaghi, "The chemistry and applications of metal-organic frameworks," *Science (1979)*, vol. 341, no. 6149, p. 1230444, 2013.

[36] S. S.-Y. Chui, S. M.-F. Lo, J. P. H. Charmant, A. G. Orpen, and I. D. Williams, "A chemically functionalizable nanoporous material [Cu3 (TMA) 2 (H2O) 3] n," *Science (1979)*, vol. 283, no. 5405, pp. 1148–1150, 1999.

[37] G. Férey *et al.*, "A Chromium Terephthalate-Based Solid with Unusually Large Pore Volumes and Surface Area," *Science (1979)*, vol. 309, no. 5743, pp. 2040–2042, Sep. 2005, doi: 10.1126/science.1116275.

[38] J. H. Cavka *et al.*, "A New Zirconium Inorganic Building Brick Forming Metal Organic Frameworks with Exceptional Stability," *J Am Chem Soc*, vol. 130, no. 42, pp. 13850–13851, Oct.

 doi:10.20944/preprints202210.0212.v1

2008, doi: 10.1021/ja8057953.

[39] W. Xiang, Y. Zhang, Y. Chen, C. Liu, and X. Tu, "Synthesis, characterization and application of defective metal–organic frameworks: current status and perspectives," *J Mater Chem A Mater*, vol. 8, no. 41, pp. 21526–21546, 2020.

[40] J. Ren *et al.*, "Structural defects in metal–organic frameworks (MOFs): Formation, detection and control towards practices of interests," *Coord Chem Rev*, vol. 349, pp. 169–197, Oct. 2017, doi: 10.1016/J.CCR.2017.08.017.

[41] N. C. Burtch, H. Jasuja, and K. S. Walton, "Water stability and adsorption in metal–organic frameworks," *Chem Rev*, vol. 114, no. 20, pp. 10575–10612, 2014.

[42] W. Xu and O. M. Yaghi, "Metal–organic frameworks for water harvesting from air, anywhere, anytime," *ACS Cent Sci*, vol. 6, no. 8, pp. 1348–1354, 2020.

[43] K. O. Kirlikovali, Z. Chen, T. Islamoglu, J. T. Hupp, and O. K. Farha, "Zirconium-Based Metal-Organic Frameworks for the Catalytic Hydrolysis of Organophosphorus Nerve Agents," *ACS Appl Mater Interfaces*, vol. 12, no. 13, pp. 14702–14720, Apr. 2020, doi: 10.1021/acsami.9b20154.

[44] J. B. DeCoste and G. W. Peterson, "Metal–organic frameworks for air purification of toxic chemicals," *Chem Rev*, vol. 114, no. 11, pp. 5695–5727, 2014.

[45] Y. Liu, A. J. Howarth, N. A. Vermeulen, S.-Y. Moon, J. T. Hupp, and O. K. Farha, "Catalytic degradation of chemical warfare agents and their simulants by metal-organic frameworks," *Coord Chem Rev*, vol. 346, pp. 101–111, 2017.

[46] N. B. Munro *et al.*, "The sources, fate, and toxicity of chemical warfare agent degradation products.," *Environ Health Perspect*, vol. 107, no. 12, pp. 933–974, 1999.

[47] T. Islamoglu *et al.*, "Metal–organic frameworks against toxic chemicals," *Chem Rev*, vol. 120, no. 16, pp. 8130–8160, 2020.

[48] K. Vellingiri, L. Philip, and K. H. Kim, "Metal–organic frameworks as media for the catalytic degradation of chemical warfare agents," *Coord Chem Rev*, vol. 353, pp. 159–179, Dec. 2017, doi: 10.1016/J.CCR.2017.10.010.

[49] S. J. Garibay, O. K. Farha, and J. B. DeCoste, "Single-component frameworks for heterogeneous catalytic hydrolysis of organophosphorous compounds in pure water," *Chemical Communications*, vol. 55, no. 49, pp. 7005–7008, 2019.

[50] W. Xu and O. M. Yaghi, "Metal–organic frameworks for water harvesting from air, anywhere, anytime," *ACS Cent Sci*, vol. 6, no. 8, pp. 1348–1354, 2020.

[51] M. J. Kalmutzki, C. S. Diercks, and O. M. Yaghi, "Metal–organic frameworks for water harvesting from air," *Advanced Materials*, vol. 30, no. 37, p. 1704304, 2018.

[52] K. Ma *et al.*, "Near-instantaneous catalytic hydrolysis of organophosphorus nerve agents with zirconium-based MOF/hydrogel composites," *Chem Catalysis*, vol. 1, no. 3, pp. 721–733, 2021.

[53] J. Castells-Gil *et al.*, "Heterometallic titanium-organic frameworks as dual-metal catalysts for synergistic non-buffered hydrolysis of nerve agent simulants," *Chem*, vol. 6, no. 11, pp. 3118–3131, 2020.

[54] R. Gil-San-Millan *et al.*, "Magnesium exchanged zirconium metal–organic frameworks with improved detoxification properties of nerve agents," *J Am Chem Soc*, vol. 141, no. 30, pp. 11801–11805, 2019.

[55] E. Geravand, F. Farzaneh, R. Gil-San-Millan, F. J. Carmona, and J. A. R. Navarro, "Mixed-Metal Cerium/Zirconium MOFs with Improved Nerve Agent Detoxification Properties," *Inorg Chem*, vol. 59, no. 22, pp. 16160–16167, 2020.

 doi:10.20944/preprints202210.0212.v1

[56] C. Montoro *et al.*, "Capture of nerve agents and mustard gas analogues by hydrophobic robust MOF-5 type metal–organic frameworks," *J Am Chem Soc*, vol. 133, no. 31, pp. 11888–11891, 2011.

[57] A. J. Howarth, M. B. Majewski, and O. K. Farha, "Metal-organic frameworks for capture and detoxification of nerve agents," *Metal-Organic Frameworks (MOFs) for Environmental Applications*, pp. 179–202, Jan. 2019, doi: 10.1016/B978-0-12-814633-0.00008-9.

[58] F.-J. Ma *et al.*, "A sodalite-type porous metal− organic framework with polyoxometalate templates: adsorption and decomposition of dimethyl methylphosphonate," *J Am Chem Soc*, vol. 133, no. 12, pp. 4178–4181, 2011.

[59] M. R. Horn *et al.*, "Polyoxometalates (POMs): From electroactive clusters to energy materials," *Energy Environ Sci*, vol. 14, no. 4, pp. 1652–1700, 2021.

[60] A. Roy, A. K. Srivastava, B. Singh, D. Shah, T. H. Mahato, and A. Srivastava, "Kinetics of degradation of sulfur mustard and sarin simulants on HKUST-1 metal organic framework," *Dalton Transactions*, vol. 41, no. 40, pp. 12346–12348, 2012.

[61] G. W. Peterson and G. W. Wagner, "Detoxification of chemical warfare agents by CuBTC," *Journal of Porous Materials*, vol. 21, no. 2, pp. 121–126, 2014.

[62] D. Denysenko, M. Grzywa, J. Jelic, K. Reuter, and D. Volkmer, "Scorpionate-type coordination in MFU-4l metal–organic frameworks: small-molecule binding and activation upon the thermally activated formation of open metal sites," *Angewandte Chemie International Edition*, vol. 53, no. 23, pp. 5832–5836, 2014.

[63] M. R. Mian *et al.*, "Catalytic degradation of an organophosphorus agent at Zn–OH sites in a metal–organic framework," *Chemistry of Materials*, vol. 32, no. 16, pp. 6998–7004, 2020.

[64] M. R. Mian *et al.*, "Insights into Catalytic Hydrolysis of Organophosphonates at M–OH Sites of Azolate-Based Metal Organic Frameworks," *J Am Chem Soc*, vol. 143, no. 26, pp. 9893–9900, 2021.

[65] D. Dang, Y. Bai, C. He, J. Wang, C. Duan, and J. Niu, "Structural and Catalytic Performance of a Polyoxometalate-Based Metal− Organic Framework Having a Lanthanide Nanocage as a Secondary Building Block," *Inorg Chem*, vol. 49, no. 4, pp. 1280–1282, 2010.

[66] L. Bromberg *et al.*, "Alkylaminopyridine-modified aluminum aminoterephthalate metal-organic frameworks as components of reactive self-detoxifying materials," *ACS Appl Mater Interfaces*, vol. 4, no. 9, pp. 4595–4602, 2012.

[67] T. Ahnfeldt *et al.*, "Synthesis and Modification of a Functionalized 3D Open-Framework Structure with MIL-53 Topology," *Inorg Chem*, vol. 48, no. 7, pp. 3057–3064, Apr. 2009, doi: 10.1021/ic8023265.

[68] T. Loiseau *et al.*, "A rationale for the large breathing of the porous aluminum terephthalate (MIL-53) upon hydration," *Chemistry–A European Journal*, vol. 10, no. 6, pp. 1373–1382, 2004.

[69] S. H. Jhung, J. Lee, J. W. Yoon, C. Serre, G. Férey, and J. Chang, "Microwave synthesis of chromium terephthalate MIL-101 and its benzene sorption ability," *Advanced Materials*, vol. 19, no. 1, pp. 121–124, 2007.

[70] M. G. Goesten *et al.*, "Molecular promoting of aluminum metal–organic framework topology MIL-101 by N, N-Dimethylformamide," *Inorg Chem*, vol. 53, no. 2, pp. 882–887, 2014.

[71] S. Wang, L. Bromberg, H. Schreuder-Gibson, and T. A. Hatton, "Organophophorous Ester Degradation by Chromium(III) Terephthalate Metal–Organic Framework (MIL-101) Chelated to *N* , *N* -Dimethylaminopyridine and Related Aminopyridines," *ACS Appl Mater Interfaces*, vol. 5,

no. 4, pp. 1269–1278, Feb. 2013, doi: 10.1021/am302359b.

[72] A. M. Rice, G. A. Leith, O. A. Ejegbavwo, E. A. Dolgopolova, and N. B. Shustova, "Heterometallic metal–organic frameworks (MOFs): the advent of improving the energy landscape," *ACS Energy Lett*, vol. 4, no. 8, pp. 1938–1946, 2019.

[73] S. R. Halper, L. Do, J. R. Stork, and S. M. Cohen, "Topological control in heterometallic metal–organic frameworks by anion templating and metalloligand design," *J Am Chem Soc*, vol. 128, no. 47, pp. 15255–15268, 2006.

[74] J. Liu *et al.*, "Recent advances of functional heterometallic-organic framework (HMOF) materials: Design strategies and applications," *Coord Chem Rev*, vol. 463, p. 214521, 2022.

[75] M. Silva and J. Baltrusaitis, "Destruction of emerging organophosphate contaminants in wastewater using the heterogeneous iron-based photo-Fenton-like process," *Journal of Hazardous Materials Letters*, vol. 2, p. 100012, Nov. 2021, doi: 10.1016/J.HAZL.2020.100012.

[76] C. Du *et al.*, "Fe-based metal organic frameworks (Fe-MOFs) for organic pollutants removal via photo-Fenton: A review," *Chemical Engineering Journal*, vol. 431, p. 133932, Mar. 2022, doi: 10.1016/J.CEJ.2021.133932.

[77] H. Fakhri, M. Farzadkia, R. Boukherroub, V. Srivastava, and M. Sillanpää, "Design and preparation of core-shell structured magnetic graphene oxide@MIL-101(Fe): Photocatalysis under shell to remove diazinon and atrazine pesticides," *Solar Energy*, vol. 208, pp. 990–1000, Sep. 2020, doi: 10.1016/J.SOLENER.2020.08.050.

[78] K. Zhang, X. Cao, Z. Zhang, Y. Cheng, and Y.-H. Zhou, "MIL-101 (Cr) with incorporated polypyridine zinc complexes for efficient degradation of a nerve agent simulant: spatial isolation of active sites promoting catalysis," *Dalton Transactions*, vol. 50, no. 6, pp. 1995–2000, 2021.

[79] Z. Chen, S. L. Hanna, L. R. Redfern, D. Alezi, T. Islamoglu, and O. K. Farha, "Reticular chemistry in the rational synthesis of functional zirconium cluster-based MOFs," *Coord Chem Rev*, vol. 386, pp. 32–49, May 2019, doi: 10.1016/J.CCR.2019.01.017.

[80] H. Furukawa *et al.*, "Water Adsorption in Porous Metal–Organic Frameworks and Related Materials," *J Am Chem Soc*, vol. 136, no. 11, pp. 4369–4381, Mar. 2014, doi: 10.1021/ja500330a.

[81] T. L. H. Doan, T. Q. Dao, H. N. Tran, P. H. Tran, and T. N. Le, "An efficient combination of Zr-MOF and microwave irradiation in catalytic Lewis acid Friedel–Crafts benzoylation," *Dalton Transactions*, vol. 45, no. 18, pp. 7875–7880, 2016, doi: 10.1039/C6DT00827E.

[82] M. J. Katz *et al.*, "Simple and Compelling Biomimetic Metal-Organic Framework Catalyst for the Degradation of Nerve Agent Simulants," *Angewandte Chemie*, vol. 126, no. 2, pp. 507–511, Jan. 2014, doi: 10.1002/ange.201307520.

[83] A. M. Ploskonka and J. B. DeCoste, "Insight into organophosphate chemical warfare agent simulant hydrolysis in metal-organic frameworks," *J Hazard Mater*, vol. 375, pp. 191–197, Aug. 2019, doi: 10.1016/J.JHAZMAT.2019.04.044.

[84] Y. Bai, Y. Dou, L.-H. Xie, W. Rutledge, J.-R. Li, and H.-C. Zhou, "Zr-based metal–organic frameworks: design, synthesis, structure, and applications," *Chem Soc Rev*, vol. 45, no. 8, pp. 2327–2367, 2016, doi: 10.1039/C5CS00837A.

[85] M. J. Katz *et al.*, "Exploiting parameter space in MOFs: a 20-fold enhancement of phosphate-ester hydrolysis with UiO-66-NH $_2$," *Chem Sci*, vol. 6, no. 4, pp. 2286–2291, 2015, doi: 10.1039/C4SC03613A.

[86] M. C. de Koning, M. van Grol, and T. Breijaert, "Degradation of Paraoxon and the Chemical Warfare Agents VX, Tabun, and Soman by the Metal–Organic Frameworks UiO-66-NH $_2$, MOF-

 doi:10.20944/preprints202210.0212.v1

808, NU-1000, and PCN-777," *Inorg Chem*, vol. 56, no. 19, pp. 11804–11809, Oct. 2017, doi: 10.1021/acs.inorgchem.7b01809.

[87] Y. Wang, S. Saebø, and C. U. Pittman, "The structure of aniline by ab initio studies," *Journal of Molecular Structure: THEOCHEM*, vol. 281, no. 2–3, pp. 91–98, Apr. 1993, doi: 10.1016/0166-1280(93)87064-K.

[88] A. H. Vahabi, F. Norouzi, E. Sheibani, and M. Rahimi-Nasrabadi, "Functionalized Zr-UiO-67 metal-organic frameworks: Structural landscape and application," *Coord Chem Rev*, vol. 445, p. 214050, Oct. 2021, doi: 10.1016/J.CCR.2021.214050.

[89] T. Islamoglu *et al.*, "Presence versus Proximity: The Role of Pendant Amines in the Catalytic Hydrolysis of a Nerve Agent Simulant," *Angewandte Chemie International Edition*, vol. 57, no. 7, pp. 1949–1953, Feb. 2018, doi: 10.1002/anie.201712645.

[90] S.-Y. Moon *et al.*, "Effective, Facile, and Selective Hydrolysis of the Chemical Warfare Agent VX Using Zr $_6$ -Based Metal–Organic Frameworks," *Inorg Chem*, vol. 54, no. 22, pp. 10829–10833, Nov. 2015, doi: 10.1021/acs.inorgchem.5b01813.

[91] M. Wahiduzzaman, S. Wang, B. J. Sikora, C. Serre, and G. Maurin, "Computational structure determination of novel metal–organic frameworks," *Chemical Communications*, vol. 54, no. 77, pp. 10812–10815, 2018.

[92] S. Wang *et al.*, "A robust zirconium amino acid metal-organic framework for proton conduction," *Nat Commun*, vol. 9, no. 1, pp. 1–8, 2018.

[93] S. S. Sandhu *et al.*, "Green MIP-202 (Zr) Catalyst: Degradation and Thermally Robust Biomimetic Sensing of Nerve Agents," *J Am Chem Soc*, vol. 143, no. 43, pp. 18261–18271, 2021.

[94] K. Y. Goud *et al.*, "Textile-based wearable solid-contact flexible fluoride sensor: Toward biodetection of G-type nerve agents," *Biosens Bioelectron*, vol. 182, p. 113172, Jun. 2021, doi: 10.1016/J.BIOS.2021.113172.

[95] Z. Chen, K. O. Kirlikovali, P. Li, and O. K. Farha, "Reticular Chemistry for Highly Porous Metal–Organic Frameworks: The Chemistry and Applications," *Acc Chem Res*, vol. 55, no. 4, pp. 579–591, 2022.

[96] Z. Chen *et al.*, "Ligand-directed reticular synthesis of catalytically active missing zirconium-based metal–organic frameworks," *J Am Chem Soc*, vol. 141, no. 31, pp. 12229–12235, 2019.

[97] T. E. Webber, W.-G. Liu, S. P. Desai, C. C. Lu, D. G. Truhlar, and R. L. Penn, "Role of a Modulator in the Synthesis of Phase-Pure NU-1000," *ACS Appl Mater Interfaces*, vol. 9, no. 45, pp. 39342–39346, 2017.

[98] P. Li *et al.*, "Synthesis of nanocrystals of Zr-based metal–organic frameworks with csq-net: significant enhancement in the degradation of a nerve agent simulant," *Chemical communications*, vol. 51, no. 54, pp. 10925–10928, 2015.

[99] R. Gil-San-Millan *et al.*, "Magnesium exchanged zirconium metal–organic frameworks with improved detoxification properties of nerve agents," *J Am Chem Soc*, vol. 141, no. 30, pp. 11801–11805, 2019.

[100] J. E. Mondloch *et al.*, "Destruction of chemical warfare agents using metal–organic frameworks," *Nat Mater*, vol. 14, no. 5, pp. 512–516, 2015.

[101] P. K. Verma *et al.*, "Controlling Polymorphism and Orientation of NU-901/NU-1000 Metal–Organic Framework Thin Films," *Chemistry of Materials*, vol. 32, no. 24, pp. 10556–10565, 2020.

[102] S. J. Garibay, I. Iordanov, T. Islamoglu, J. B. DeCoste, and O. K. Farha, "Synthesis and functionalization of phase-pure NU-901 for enhanced CO 2 adsorption: the influence of a

zirconium salt and modulator on the topology and phase purity," *CrystEngComm*, vol. 20, no. 44, pp. 7066–7070, 2018.

[103] Z. Chen, T. Islamoglu, and O. K. Farha, "Toward base heterogenization: A zirconium metal–organic framework/dendrimer or polymer mixture for rapid hydrolysis of a nerve-agent simulant," *ACS Appl Nano Mater*, vol. 2, no. 2, pp. 1005–1008, 2019.

[104] H. J. Park *et al.*, "Synthesis of a Zr-Based Metal–Organic Framework with Spirobifluorenetetrabenzoic Acid for the Effective Removal of Nerve Agent Simulants," *Inorg Chem*, vol. 56, no. 20, pp. 12098–12101, Oct. 2017, doi: 10.1021/acs.inorgchem.7b02022.

[105] H.-Q. Zheng *et al.*, "MOF-808: a metal–organic framework with intrinsic peroxidase-like catalytic activity at neutral pH for colorimetric biosensing," *Inorg Chem*, vol. 57, no. 15, pp. 9096–9104, 2018.

[106] S. Y. Moon, Y. Liu, J. T. Hupp, and O. K. Farha, "Instantaneous hydrolysis of nerve-agent simulants with a six-connected zirconium-based metal-organic framework," *Angewandte Chemie - International Edition*, vol. 54, no. 23, 2015, doi: 10.1002/anie.201502155.

[107] M. C. de Koning, C. Vieira Soares, M. van Grol, R. P. T. Bross, and G. Maurin, "Effective Degradation of Novichok Nerve Agents by the Zirconium Metal–Organic Framework MOF-808," *ACS Appl Mater Interfaces*, vol. 14, no. 7, pp. 9222–9230, Feb. 2022, doi: 10.1021/acsami.1c24295.

[108] D. Steindl *et al.*, "Novichok nerve agent poisoning," *The Lancet*, vol. 397, no. 10270, pp. 249–252, 2021.

[109] Z. Chen *et al.*, "Integration of Metal–Organic Frameworks on Protective Layers for Destruction of Nerve Agents under Relevant Conditions," *J Am Chem Soc*, vol. 141, no. 51, pp. 20016–20021, Dec. 2019, doi: 10.1021/jacs.9b11172.

[110] H.-B. Luo, A. J. Castro, M. C. Wasson, W. Flores, O. K. Farha, and Y. Liu, "Rapid, Biomimetic Degradation of a Nerve Agent Simulant by Incorporating Imidazole Bases into a Metal–Organic Framework," *ACS Catal*, vol. 11, no. 3, pp. 1424–1429, 2021.

[111] K. Ma *et al.*, "Near-instantaneous catalytic hydrolysis of organophosphorus nerve agents with zirconium-based MOF/hydrogel composites," *Chem Catalysis*, vol. 1, no. 3, pp. 721–733, Aug. 2021, doi: 10.1016/J.CHECAT.2021.06.008.

[112] N. Y. Huang, J. Gu, D. Chen, and Q. Xu, "MOF/hydrogel catalysts for efficient nerve-agent degradation," *Chem Catalysis*, vol. 1, no. 3, pp. 502–504, Aug. 2021, doi: 10.1016/J.CHECAT.2021.07.010.

[113] E. Geravand, F. Farzaneh, R. Gil-San-Millan, F. J. Carmona, and J. A. R. Navarro, "Mixed-Metal Cerium/Zirconium MOFs with Improved Nerve Agent Detoxification Properties," *Inorg Chem*, vol. 59, no. 22, pp. 16160–16167, 2020.

[114] Y. Zhang *et al.*, "A Flexible Metal–Organic Framework with 4-Connected Zr $_6$ Nodes," *J Am Chem Soc*, vol. 140, no. 36, pp. 11179–11183, Sep. 2018, doi: 10.1021/jacs.8b06789.

[115] C. Liu, J. Wang, J. Wan, and C. Yu, "MOF-on-MOF hybrids: Synthesis and applications," *Coord Chem Rev*, vol. 432, p. 213743, Apr. 2021, doi: 10.1016/J.CCR.2020.213743.

[116] M. Zhao *et al.*, "Metal–organic frameworks as selectivity regulators for hydrogenation reactions," *Nature*, vol. 539, no. 7627, pp. 76–80, Nov. 2016, doi: 10.1038/nature19763.

[117] Y. Gu, Y. Wu, L. Li, W. Chen, F. Li, and S. Kitagawa, "Controllable Modular Growth of Hierarchical MOF-on-MOF Architectures," *Angewandte Chemie International Edition*, vol. 56, no. 49, pp. 15658–15662, Dec. 2017, doi: 10.1002/anie.201709738.

 doi:10.20944/preprints202210.0212.v1

[118] M. B. Majewski, H. Noh, T. Islamoglu, and O. K. Farha, “NanoMOFs: little crystallites for substantial applications,” *J Mater Chem A Mater*, vol. 6, no. 17, pp. 7338–7350, 2018.